FZJ-IKP(TH)-1998-03 hep-ph/9803266

arXiv:hep-ph/9803266v2 26 Aug 1998

Pion–nucleon scattering in chiral perturbation theory I: Isospin–symmetric case[#1]

Nadia Fettes[‡#2], Ulf-G. Meißner[‡#3], Sven Steininger[‡,†#4]

[‡]FZ Jülich, IKP (Theorie), D–52425 Jülich, Germany

[†]Universität Bonn, ITKP, Nussallee 14-16, D–53115 Bonn, Germany

Abstract

We construct the complete effective chiral pion–nucleon Lagrangian to third order in small momenta based on relativistic chiral perturbation theory. We then perform the so–called heavy baryon limit and construct all terms up–to–and–including order $1/m^2$ with fixed and free coefficients. As an application, we discuss in detail pion–nucleon scattering. In particular, we show that for this process and to third order, the $1/m$ expansion of the Born graphs calculated relativistically can be recovered exactly in the heavy baryon approach without any additional momentum–dependent wave function renormalization. We fit various empirical phase shifts for pion laboratory momenta between 50 and 100 MeV. This leads to a satisfactory description of the phase shifts up to momenta of about 200 MeV. We also predict the threshold parameters, which turn out to be in good agreement with the dispersive analysis. In particular, we can sharpen the prediction for the isovector S–wave scattering length, $0.083\, M_\pi^{-1} \leq a_{0+}^- \leq 0.093\, M_\pi^{-1}$. We also consider the subthreshold parameters and give a short comparison to other calculations of πN scattering in chiral perturbation theory or modifications thereof.

Accepted for publication in Nuclear Physics A

[#1]Work supported in part by funds provided by the Graduiertenkolleg "Die Erforschung subnuklearer Strukturen der Materie" at Bonn University.

[#2]email: N.Fettes@fz-juelich.de

[#3]email: Ulf-G.Meissner@fz-juelich.de

[#4]email: sven@pythia.itkp.uni-bonn.de

1 Introduction and summary

One of the outstanding problems in nuclear and particle physics is to understand quantitatively the violation of isospin symmetry. In a world of strong interactions only, the light quark mass difference $m_d - m_u$ is the only mechanism for isospin violation. In the real world, the situation is complicated by the electromagnetic interactions, which clearly do not conserve isospin (the photon couples to the electric charge). With the advent of high–precision data on pionic hydrogen and deuterium at PSI [1] and neutral pion photoproduction data from MAMI [2] and SAL [3], novel interest has been spurred in separating electromagnetic effects and trying to filter out isospin violating contributions. In addition, in the framework of some models it has been claimed that the presently available pion–nucleon data basis exhibits isospin violation of the order of a few percent [4][5]. However, to really pin down isospin breaking due to the light quark mass difference, one needs a machinery that allows to *simultaneously* and *consistently* treat the electromagnetic and the strong contributions. The only framework known at present allowing to do just that is (heavy baryon) chiral perturbation theory (HBCHPT). It is based on a consistent power counting scheme which allows to order the various terms according to the number of derivatives and/or meson mass insertions. This defines the so–called chiral dimension corresponding to the number of derivatives and/or pion mass insertions, with the pertinent small parameters collectively denoted by q. For the pion–nucleon system, the leading term is of dimension one and loops start to contribute at two orders higher (in the heavy fermion formulation). HBCHPT has become a precision tool to investigate a rich variety of processes in the pion–nucleon system, in particular reactions involving real and virtual photons (for a review, see [6] and an update is given in [7]).

Over the years, Bernard et al. have investigated aspects of pion–nucleon scattering, in particular the chiral corrections to the S–wave scattering lengths [8, 9], the size of the remainder at the Cheng-Dashen point [10] and the strength of the dimension two low–energy constants (LECs) extracted from πN threshold and subthreshold parameters, that do not depend on dimension three LECs [11]. Most of these calculations were done in the one–loop approximation, some to order q^3 and some to order q^4.[#5] The complete one–loop amplitude to order q^3 was first given by Mojžiš [12] based on the effective Lagrangian constructed in [13]. In ref.[12], the Karlsruhe–Helsinki [14] threshold parameters together with the pion–nucleon coupling constant and the πN σ–term were used to pin down the various LECs of dimension two and three. The resulting phase shifts were later evaluated for pion kinetic laboratory energies up to 140 MeV in [15]. Simultaneously, the effective Lagrangian including also virtual photons was developed in [16] to third order in small momenta (counting also the electric charge e as an additional small parameter) and isospin–violating effects for the scattering of neutral pions off nucleons and in the σ–term were evaluated. This extended effective Lagrangian was based on the pion–nucleon Lagrangian as formulated in the review [6]. To allow for an easier comparison with the various calculations performed in that basis, we construct here the corresponding third order effective Lagrangian. This extends the work of Ecker and Mojžiš [13] since we explicitely work out the various $1/m$ corrections to the dimension three terms and do not

[#5] Note that due to the appearance of odd and even powers in the effective pion–nucleon Lagrangian, the N–loop order consists of terms of order q^{2N+1} and q^{2N+2}.

absorb them in the corresponding LECs (as done in [13]). We also fill in some details on the construction of the effective Lagrangian which have not yet appeared in the literature. In the second part of this investigation, we use pion–nucleon phase shifts in the low–energy region as given by different analyses to pin down our LECs. We argue that considering the present status in the pion–nucleon scattering data basis, this is a more stable procedure than the one used before. In particular, it allows to extract the theoretical errors related to the variations in the empirical input. This is of utmost importance if one intends to continue these studies to next order and work out the size and origin of the isospin violation.

The pertinent results of this investigation can be summarized as follows:

(i) We have constructed the minimal pion–nucleon Lagrangian at third order in the chiral expansion, including all corrections arising from the expansion in the inverse nucleon mass (with fixed coefficients as well as dimension two LECs). We have also enumerated the purely divergent terms which arise from the evaluation of the one–loop generating functional to one loop and order q^3. At third order, the effective Lagrangian has 23 terms with LECs. Only 14 of these have a non–vanishing β–function. This extends the result obtained in [13].

(ii) We have constructed the complete amplitude for elastic pion–nucleon scattering to order q^3. Our loop contribution agrees exactly with the one given previously [12, 11]. For the tree graphs, we have shown the exact equivalence between the $1/m$ expansion of the result obtained in the relativistic theory and the one calculated directly in the heavy baryon approach, provided one does not expand the normalization factor of the nucleon spinors.

(iii) We have fitted the two S– and four P–wave partial wave amplitudes for three different sets of available pion–nucleon phase shifts at intermediate energies (typically in the range of 50 to 100 MeV pion momentum in the laboratory frame). This allows to predict the phases at *lower* and at *higher* energies, in particular the (sub)threshold parameters (scattering lengths and effective ranges). By this fitting procedure we can determine the four dimension two LECs $c_{1,2,3,4}$ and five (combinations) of dimension three LECs. The numerical values for the LECs $c_{2,3,4}$ are in good agreement with previous determinations from threshold and subthreshold parameters alone [11, 12]. Consequently, the numerical values of these LECs can be understood by resonance exchange saturation, see [11]. The LEC c_1, which is directly related to the σ–term, comes out larger than before. We show, however, that the fits are not very sensitive to its actual value and one thus can not pin down the σ–term at this order in the chiral expansion. The dimension three LECs have "natural" size.

(iv) We have evaluated the threshold parameters using the one–loop amplitude for the extrapolation. The results are fairly stable for the various fits and, if applicable, comparable to the results based on dispersion theory. As already known, the isoscalar S–wave scattering length can not be determined precisely to this order, but we give an improved prediction for the isovector one, $0.083\, M_\pi^{-1} \leq a_{0+}^- \leq 0.093\, M_\pi^{-1}$. This value is in good agreement with recent determinations from the strong interaction level shift in pionic atoms measured at PSI [1] and with values extracted from phase shift analyses.

2 Construction of the effective Lagrangian

In this section, we give a detailed exposition how to arrive at the dimension three effective chiral pion–nucleon Lagrangian. While parts of the final result have already been given by Ecker and Mojžiš [13], we fill in the necessary details and also work in the basis of the review [6], which is most convenient for comparison with earlier work on photoproduction, Compton scattering and so on. In particular, in [13] the $1/m$ corrections appearing at third order were always subsumed in the LECs (whenever possible). While this is a legitimate procedure, we prefer these corrections to be separated, in particular, if one wishes to estimate the corresponding LECs via resonance exchange or some other model. The construction of $\mathcal{L}_{\pi N}^{(3)}$ is done in five steps. These are: (1) enumeration of the building blocks for relativistic spin–1/2 fields chirally coupled to pions and external sources, (2) saturation of the free Lorentz indices by elements of the underlying Clifford algebra and other operators of chiral dimension zero (and one), (3) construction of the overcomplete relativistic Lagrangian, (4) reduction of terms by use of various relations and (5) performing the non–relativistic limit and working out the $1/m$ corrections by use of the path integral [17]. The details will be spelled out in the following paragraphs.[#6] The reader more interested in the application to pion–nucleon scattering might skip this section.

2.1 Effective theory with relativistic nucleons

The starting point of our approach is to construct the most general chiral invariant Lagrangian built from pions, nucleons and external scalar, pseudoscalar, vector and axial–vector sources. The Goldstone bosons are collected in a 2×2 matrix-valued field $U(x) = u^2(x)$. The nucleons are described by structureless relativistic spin-$\frac{1}{2}$ particles, the spinors being denoted by $\Psi(x)$. The effective theory admits a low energy expansion, i.e. the corresponding effective Lagrangian can be written as (for more details and references, see e.g. [6])

$$\mathcal{L}_{\rm eff} = \mathcal{L}_{\pi\pi}^{(2)} + \mathcal{L}_{\pi\pi}^{(4)} + \mathcal{L}_{\pi N}^{(1)} + \mathcal{L}_{\pi N}^{(2)} + \mathcal{L}_{\pi N}^{(3)} + \dots \ , \tag{2.1}$$

where the ellipsis denotes terms of higher order. For the explicit form of the meson Lagrangian and the dimension one and two pion–nucleon terms, we refer to ref.[6]. We remark that to be precise, the various parameters like $g_A, m, \dots$ appearing in the effective Lagrangian have to be taken in the chiral SU(2) limit ($m_u = m_d = 0$, m_s fixed) and should be denoted as $\mathring{g}_A, \mathring{m}, \dots$. Throughout this section, we will not specify this but it should be kept in mind. In what follows, we are mostly interested in the third order terms collected in $\mathcal{L}_{\pi N}^{(3)}$. To construct these, we use the standard methods of non–linearly realized chiral symmetry. From the external sources, we construct the following building

[#6] After submission of this paper, another manuscript which also deals with this topic appeared [43].

blocks starting with the covariant derivative D_μ (here and in what follows, A denotes an arbitrary 2×2 matrix):

$$
\begin{aligned}
D_\mu A &= \partial_\mu A + \Gamma_\mu A \ , && (2.2)\\
\Gamma_\mu &= \frac{1}{2}\,[u^\dagger, \partial_\mu u] - \frac{i}{2}\,u^\dagger r_\mu u - \frac{i}{2}\,u l_\mu u^\dagger \ , && (2.3)\\
u_\mu &= i\left(\partial_\mu u\, u^\dagger + u^\dagger \partial_\mu u - i\, u^\dagger r_\mu u + i\, u l_\mu u^\dagger\right) \ , && (2.4)\\
r_\mu &= v_\mu + a_\mu \ , \quad l_\mu = v_\mu - a_\mu \ , && (2.5)\\
F^\pm_{\mu\nu} &= u^\dagger F^R_{\mu\nu} u \pm u F^L_{\mu\nu} u^\dagger \ , && (2.6)\\
F^L_{\mu\nu} &= \partial_\mu l_\nu - \partial_\nu l_\mu - i\,[l_\mu, l_\nu] \ , && (2.7)\\
F^R_{\mu\nu} &= \partial_\mu r_\nu - \partial_\nu r_\mu - i\,[r_\mu, r_\nu] \ , && (2.8)\\
\chi_\pm &= u^\dagger \chi u^\dagger \pm u \chi^\dagger u \ , && (2.9)
\end{aligned}
$$

and we employ the following definition for traceless operators ('$\langle \ldots \rangle$' denotes the trace in flavor space)

$$
\hat{A} = A - \frac{1}{2}\,\langle A \rangle \ . \tag{2.10}
$$

Here, $\chi(x) = s(x) + ip(x)$ includes the explicit chiral symmetry breaking through the small current quark masses, $s(x) = B\,\mathrm{diag}(m_u, m_d) + \ldots$ and

$$
B = \frac{|\langle 0|\bar{q}q|0\rangle|}{F_\pi^2} \ , \tag{2.11}
$$

with F_π the (weak) pion decay constant and the scalar quark condensate is the order parameter of the chiral symmetry breaking. We assign the following chiral dimensions to the pertinent fields and operators:

$$
\begin{aligned}
&U(x), \Psi(x), \partial_\mu \Psi(x) = \mathcal{O}(1) \ , \\
&\partial_\mu U(x), u_\mu(x), l_\mu(x), r_\mu(x) = \mathcal{O}(q) \ , \\
&s(x), p(x), \chi_\pm, F^\pm_{\mu\nu}(x), F^{L,R}_{\mu\nu}(x) = \mathcal{O}(q^2) \ ,
\end{aligned} \tag{2.12}
$$

which amounts to the so–called large condensate scenario of the spontaneous chiral symmetry violation, $B \gg F_\pi$.[#7] Here, q denotes a genuine small momentum or meson mass with respect to the typical hadronic scale of about 1 GeV. Furthermore, in the following we will make use of the operator relations

$$
\begin{aligned}
[D_\mu, D_\nu] &= \frac{1}{4}\,[u_\mu, u_\nu] - \frac{i}{2}\,F^+_{\mu\nu} \ , && (2.13)\\
F^-_{\mu\nu} &= [D_\mu, u_\nu] - [D_\nu, u_\mu] \ . && (2.14)
\end{aligned}
$$

Note that if we are only dealing with photons (A_μ) as external fields, $F^\pm_{\mu\nu}$ simplifies to $F^\pm_{\mu\nu} = (\partial_\mu A_\nu - \partial_\nu A_\mu)(uQu^\dagger \pm u^\dagger Q u)$ with $Q = e\,\mathrm{diag}(1,0)$ the nucleon charge matrix. For

[#7] For the small B scenario, one would have to count $s(x)$ and $p(x)$ as order q.

a consistent counting scheme including also virtual photons [18], one has to consider the electric charge e as another small quantity of order q.

There is one subtlety in the fully relativistic theory, namely the appearance of the large nucleon mass scale (to be precise, the mass of the nucleon in the chiral limit) [19]. Therefore any covariant derivative D_μ counts as order q^0. Formally, one could thus construct terms of the type $\bar{\Psi}\ldots D^{38}\Psi$. To avoid this, consider the covariant derivative only as a building block when it acts on operators sandwiched between the spinors (the only exception to this rule is the lowest order Lagrangian). The pertinent terms involving D_μ acting on the nucleon fields, which are all of chiral dimension zero (or one), are given together with the elements of the Clifford algebra in the next paragraph since they are used to saturate the free Lorentz indices of the building blocks. In this way, one avoids from the beginning all terms with an arbitrary large number of D_μ's, which are formally allowed. With that in mind, the possible building blocks at orders q, q^2 and q^3 are enumerated in table 1 (also given are the respective charge conjugation, C, and parity, P, assignments). Of course, hermiticity has to be assured by appropriate factors of i and combinations of

Operator	C	P		Operator	C	P
u_μ	$+$	$-$		$[D_\mu, \langle\chi_+\rangle]$	$+$	$+$
	$\mathcal{O}(q^2)$			$\langle\hat{\chi}_- u_\mu\rangle$	$+$	$+$
$\hat{\chi}_+$	$+$	$+$		$\langle\chi_-\rangle u_\mu$	$+$	$+$
$\langle\chi_+\rangle$	$+$	$+$		$[\chi_-, u_\mu]$	$-$	$+$
$\hat{\chi}_-$	$+$	$-$		$[D_\mu, \hat{\chi}_-]$	$+$	$-$
$\langle\chi_-\rangle$	$+$	$-$		$[D_\mu, \langle\chi_-\rangle]$	$+$	$-$
$\langle u_\mu u_\nu\rangle$	$+$	$+$		$\langle u_\mu u_\nu\rangle u_\lambda$	$+$	$-$
$[u_\mu, u_\nu]$	$-$	$+$		$\langle u_\mu [u_\nu, u_\lambda]\rangle$	$-$	$-$
$[D_\mu, u_\nu]$	$+$	$-$		$\langle [D_\mu, u_\nu] u_\lambda\rangle$	$+$	$+$
$\hat{F}^+_{\mu\nu}$	$-$	$+$		$[[D_\mu, u_\nu], u_\lambda]$	$-$	$+$
$\langle F^+_{\mu\nu}\rangle$	$-$	$+$		$[D_\mu, [D_\nu, u_\lambda]]$	$+$	$-$
	$\mathcal{O}(q^3)$			$\langle \hat{F}^+_{\mu\nu} u_\lambda\rangle$	$-$	$-$
$\langle\hat{\chi}_+ u_\mu\rangle$	$+$	$-$		$\langle F^+_{\mu\nu}\rangle u_\lambda$	$-$	$-$
$\langle\chi_+\rangle u_\mu$	$+$	$-$		$[\hat{F}^+_{\mu\nu}, u_\lambda]$	$+$	$-$
$[\chi_+, u_\mu]$	$-$	$-$		$[D_\lambda, \hat{F}^+_{\mu\nu}]$	$-$	$+$
$[D_\mu, \hat{\chi}_+]$	$+$	$+$		$[D_\lambda, \langle F^+_{\mu\nu}\rangle]$	$-$	$+$

Table 1: Building blocks of the relativistic pion–nucleon effective theory. Note that the covariant derivative does not act on the nucleon spinors not shown.

terms. For the reasons given above, we treat the covariant derivative acting on nucleons separately and also the nucleon mass term, which is formally of order q^0. Note, however, that the operator $i\not{D} - m$ is proportional to the nucleon three–momentum, which can be small.

Now we have to construct the elements of the Clifford algebra and all other operators of dimension zero/one to contract the Lorentz indices of the building blocks. Consider first all operators constructed from γ matrices, the metric tensor and the totally antisymmetric tensor in $d = 4$ according to the number of free indices, called N_I:

$$\begin{aligned} N_0 \ : \quad & 1 \ , \ \gamma_5 \ ; \quad N_1 : \quad \gamma_\mu \ , \ \gamma_\mu\gamma_5 \ ; \quad N_2 : \quad g_{\mu\nu} \ , \ g_{\mu\nu}\gamma_5 \ , \ \sigma_{\mu\nu} \ , \ \sigma_{\mu\nu}\gamma_5 \ ; \\ N_3 \ : \quad & g_{\mu\nu}\gamma_\lambda \ , \ g_{\mu\nu}\gamma_\lambda\gamma_5 \ , \ \epsilon_{\mu\nu\lambda\alpha}\gamma^\alpha \ , \ \epsilon_{\mu\nu\lambda\alpha}\gamma^\alpha\gamma_5 \ . \end{aligned} \tag{2.15}$$

Similarly, the terms involving the covariant derivative read

$$N_1 : \ D_\mu \ ; \quad N_2 : \ \{D_\mu, D_\nu\} \ ; \quad N_3 : \ D_\mu D_\nu D_\lambda + \text{permutations} \ . \tag{2.16}$$

It is important to note that γ_5 and $g_{\mu\nu}\gamma_5$ have chiral dimension one because they only connect the large to the small components and thus appear first at order $1/m$. Terms with more D_μ's can always be reduced to the ones listed in eqs.(2.15,2.16) or they only contribute to higher orders by use of the baryon eom,

$$i\not{D}\Psi = \left(m + \frac{g_A}{2}\gamma_5 \not{u}\right)\Psi + \mathcal{O}(q^2) \ . \tag{2.17}$$

To be specific, consider as an example an operator O of dimension three constructed from the above building blocks and properly contracted to be a scalar with $PC = ++$ contributing as $\bar\Psi\, O\, \Psi$ to the effective Lagrangian. As stated before, the covariant derivative acting on a nucleon spinor is of order q^0, i.e. one could have a term like $\bar\Psi\, O\, D^2\, \Psi + \text{h.c.}$, which is also of dimension three and commensurate with all symmetries. However, it contributes only to higher orders as can be seen from the following chain of manipulations:

$$\begin{aligned} \bar\Psi\, O\, D^2\, \Psi &= \bar\Psi\, O\, g_{\mu\nu} D^\mu D^\nu\, \Psi \\ &= \bar\Psi\, O\ \not{D}\not{D}\ \Psi - i\,\bar\Psi\, O\, \sigma^{\mu\nu} D_\mu D_\nu\, \Psi \\ &= \bar\Psi\, O\ \not{D}\not{D}\ \Psi - \frac{i}{2}\,\bar\Psi\, O\, \sigma^{\mu\nu}[D_\mu, D_\nu]\, \Psi \ . \end{aligned} \tag{2.18}$$

Through a repeated use of the nucleon eom, the first term on the r.h.s. of eq.(2.18) amounts to three terms with coefficents m^2, $m\, g_A$ and g_A^2, in order. While the first of these can simply be absorbed in the LEC accompanying the original term $\bar\Psi O \Psi$, the other two start to contribute at order four and five, respectively. Similarly, the second term on the r.h.s. of eq.(2.18) leads to a dimension five operator by use of eq.(2.13). Equivalently, one can use field transformations to get rid off these terms. This somewhat more elegant method is discussed in detail in appendix A.

It is now straightforward to combine the building blocks with the operators to construct the effective Lagrangian. One just has to multiply the various operators so that the result has $J^{PC} = 0^{++}$. This gives

$$\mathcal{L}_{\pi N}^{(3)} = \sum_{i=1}^{51} \bar\Psi\, O_i^{(3)}\, \Psi \quad , \tag{2.19}$$

where the $O_i^{(3)}$ are monomials in the fields of chiral dimension three. The full list of terms is given in [20]. At this stage, the Lagrangian is over–complete. All terms are allowed by the symmetries, but they are not all independent. While one could work with such an over–complete set, it is more economical to reduce it to the minimal number of independent terms.

Let us now show how one can reduce the number of terms in $\mathcal{L}_{\pi N}^{(3)}$. To be specific, consider the term $\bar\Psi\,\gamma_5\,\gamma_\mu\,[iD_\mu,\chi_-]\,\Psi$. Performing partial integrations, we can reshuffle the covariant derivative to the extreme left and and right,

$$\bar\Psi\,\gamma_5\,\gamma_\mu\,[iD_\mu,\chi_-]\,\Psi = -\bar\Psi\,i\,\overleftarrow{D}_\mu\;\gamma_5\,\gamma_\mu\,\chi_-\,\Psi - \bar\Psi\,\gamma_5\,\gamma_\mu\,\chi_-\,iD_\mu\,\Psi\;\;. \tag{2.20}$$

Using now the eom for Ψ, eq.(2.17), and the one for $\bar\Psi$, this can be cast into the form

$$\bar\Psi\,\gamma_5\,\gamma_\mu\,[iD_\mu,\chi_-]\,\Psi = -2m\,\bar\Psi\,\gamma_5\;\chi_-\,\Psi + \frac{g_A}{2}\,\bar\Psi\,[\not{u},\chi_-]\,\Psi + \mathcal{O}(q^4) \tag{2.21}$$

and these are terms which already exist at dimension three, i.e. the term under consideration can be absorbed in the structure of these two terms. By use of the relations,[#8]

$$\begin{aligned}
\bar\Psi A^\mu i\,D_\mu\Psi + \text{h.c.} &\doteq 2m\,\bar\Psi\gamma_\mu A^\mu\Psi\;, &(2.22)\\
\bar\Psi A^{\mu\nu} D_\nu D_\mu\Psi + \text{h.c.} &\doteq -i\,m\left(\bar\Psi\gamma_\mu A^{\mu\nu} D_\nu\Psi + \text{h.c.}\right)\;, &(2.23)\\
\bar\Psi A^{\mu\nu\lambda} i\,D_\lambda D_\nu D_\mu\Psi + \text{h.c.} &\doteq m\left(\bar\Psi\gamma_\mu A^{\mu\nu\lambda} D_\lambda D_\nu\Psi + \text{h.c.}\right)\;, &(2.24)\\
\bar\Psi\gamma_5\gamma_\lambda A^{\mu\lambda} D_\mu\Psi + \text{h.c.} &\doteq 2m\bar\Psi\gamma_5\sigma_{\mu\lambda}A^{\mu\lambda}\Psi + \left(\bar\Psi\gamma_5\gamma_\mu A^{\mu\lambda} D_\lambda\Psi + \text{h.c.}\right)\;, &(2.25)\\
\bar\Psi\gamma_5\gamma_\lambda A^{\mu\lambda\alpha} D_\alpha D_\mu\Psi + \text{h.c.} &\doteq m\left(\bar\Psi\gamma_5\sigma_{\mu\lambda}A^{\mu\lambda\alpha} D_\alpha\Psi + \text{h.c.}\right)\\
&+ \left(\bar\Psi\gamma_5\gamma_\mu A^{\mu\lambda\alpha} D_\alpha D_\lambda\Psi + \text{h.c.}\right)\;, &(2.26)\\
\bar\Psi\sigma_{\alpha\beta}A^{\alpha\beta\mu} i\,D_\mu\Psi + \text{h.c.} &\doteq 2m\bar\Psi\epsilon_{\alpha\beta\mu\nu}\gamma_5\gamma^\nu A^{\alpha\beta\mu}\Psi - \left(\bar\Psi\sigma_{\beta\mu}A^{\alpha\beta\mu} i\,D_\alpha\Psi + \text{h.c.}\right)\\
&+ \left(\bar\Psi\sigma_{\alpha\mu}A^{\alpha\beta\mu} i\,D_\beta\Psi + \text{h.c.}\right)\;, &(2.27)\\
\bar\Psi\gamma_5\sigma_{\alpha\beta}A^{\alpha\beta\mu} D_\mu\Psi + \text{h.c.} &\doteq -2m\bar\Psi\gamma_5\gamma^\beta A^{\mu\beta\mu}\Psi - \left(\bar\Psi\gamma_5\sigma_{\beta\mu}A^{\alpha\beta\mu} D_\alpha\Psi + \text{h.c.}\right)\\
&+ 2m\bar\Psi\gamma_5\gamma^\alpha A^{\alpha\mu\mu}\Psi + \left(\bar\Psi\gamma_5\sigma_{\alpha\mu}A^{\alpha\beta\mu} D_\beta\Psi + \text{h.c.}\right)\;, &(2.28)\\
\bar\Psi\gamma_\mu[iD^\mu, A]\Psi &\doteq \frac{g_A}{2}\bar\Psi\gamma^\mu\gamma_5[A,u_\mu]\Psi\;, &(2.29)\\
\bar\Psi\gamma_5\gamma_\mu[iD^\mu, A]\Psi &\doteq -2m\bar\Psi\gamma_5 A\Psi - \frac{g_A}{2}\bar\Psi\gamma^\mu[A,u_\mu]\Psi\;, &(2.30)
\end{aligned}$$

one can reduce the 51 terms down to 23 independent ones. The form of the Lagrangian with independent terms only is called the "minimal" one. This minimal Lagrangian is

[#8] Here, the symbol $\doteq$ means equal up to terms of higher order. For example, if A_1 is an operator of dimension three, $A_1 \doteq A_2$ stands for $A_1 = A_2 + \mathcal{O}(q^n)$, $n \geq 4$.

given by:

$$
\begin{aligned}
\mathcal{L}_{\pi N}^{\rm min} &= \mathcal{L}_{\pi N}^{(1)} + \mathcal{L}_{\pi N}^{(2,\rm min)} + \mathcal{L}_{\pi N}^{(3,\rm min)} \ , \\
\mathcal{L}_{\pi N}^{(2,\rm min)} &= \bar\Psi \Big\{ c_1 \, \langle \chi_+ \rangle - \frac{c_2}{8m^2} \Big(\langle u_\mu u_\nu \rangle \{ D^\mu, D^\nu \} + \text{h.c} \Big) + \frac{c_3}{2} \langle u^2 \rangle \\
&\quad + \frac{i\, c_4}{4} \sigma^{\mu\nu} [u_\mu, u_\nu] + c_5 \, \hat\chi_+ + \frac{c_6}{8m} \sigma^{\mu\nu} F_{\mu\nu}^+ + \frac{c_7}{8m} \sigma^{\mu\nu} \langle F_{\mu\nu}^+ \rangle \Big\} \Psi \qquad , \\
\mathcal{L}_{\pi N}^{(3,\rm min)} &= \bar\Psi \Big\{ - \frac{d_1}{2m} \Big([u_\mu, [D_\nu, u^\mu]] D^\nu + \text{h.c.} \Big) - \frac{d_2}{2m} \Big([u_\mu, [D^\mu, u_\nu]] D^\nu + \text{h.c.} \Big) \\
&\quad + \frac{d_3}{12 m^3} \Big([u_\mu, [D_\nu, u_\lambda]] (D^\mu D^\nu D^\lambda + \text{sym.}) + \text{h.c.} \Big) \\
&\quad - \frac{d_4}{2m} \Big(\epsilon^{\mu\nu\alpha\beta} \langle u_\mu u_\nu u_\alpha \rangle D_\beta + \text{h.c.} \Big) + \frac{i\, d_5}{2m} \Big([\chi_-, u_\mu] D^\mu + \text{h.c.} \Big) \\
&\quad + \frac{i\, d_6}{2m} \Big([D^\mu, \hat F_{\mu\nu}^+] D^\nu + \text{h.c.} \Big) + \frac{i\, d_7}{2m} \Big([D^\mu, \langle F_{\mu\nu}^+ \rangle] D^\nu + \text{h.c.} \Big) \\
&\quad + \frac{i\, d_8}{2m} \Big(\epsilon^{\mu\nu\alpha\beta} \langle \hat F_{\mu\nu}^+ u_\alpha \rangle D_\beta + \text{h.c.} \Big) + \frac{i\, d_9}{2m} \Big(\epsilon^{\mu\nu\alpha\beta} \langle F_{\mu\nu}^+ \rangle u_\alpha D_\beta + \text{h.c.} \Big) \\
&\quad + \frac{d_{10}}{2} \gamma^\mu \gamma_5 \langle u^2 \rangle u_\mu + \frac{d_{11}}{2} \gamma^\mu \gamma_5 \langle u_\mu u_\nu \rangle u^\nu - \frac{d_{12}}{8m^2} \Big(\gamma^\mu \gamma_5 \langle u_\nu u_\lambda \rangle u_\mu \{ D^\nu, D^\lambda \} + \text{h.c.} \Big) \\
&\quad - \frac{d_{13}}{8m^2} \Big(\gamma^\mu \gamma_5 \langle u_\mu u_\nu \rangle u_\lambda \{ D^\nu, D^\lambda \} + \text{h.c.} \Big) + \frac{i\, d_{14}}{4m} \Big(\sigma^{\mu\nu} \langle [D_\lambda, u_\mu] u_\nu \rangle D^\lambda + \text{h.c.} \Big) \\
&\quad + \frac{i\, d_{15}}{4m} \Big(\sigma^{\mu\nu} \langle u_\mu [D_\nu, u_\lambda] \rangle D^\lambda + \text{h.c.} \Big) + \frac{d_{16}}{2} \gamma^\mu \gamma_5 \langle \chi_+ \rangle u_\mu + \frac{d_{17}}{2} \gamma^\mu \gamma_5 \langle \chi_+ u_\mu \rangle \\
&\quad + \frac{i\, d_{18}}{2} \gamma^\mu \gamma_5 [D_\mu, \chi_-] + \frac{i\, d_{19}}{2} \gamma^\mu \gamma_5 [D_\mu, \langle \chi_- \rangle] \\
&\quad - \frac{i\, d_{20}}{8m^2} \Big(\gamma^\mu \gamma_5 [\hat F_{\mu\nu}^+, u_\lambda] \{ D^\nu, D^\lambda \} + \text{h.c.} \Big) + \frac{i\, d_{21}}{2} \gamma^\mu \gamma_5 [\hat F_{\mu\nu}^+, u^\nu] \\
&\quad + \frac{d_{22}}{2} \gamma^\mu \gamma_5 [D^\nu, F_{\mu\nu}^-] + \frac{d_{23}}{2} \epsilon^{\mu\nu\alpha\beta} \gamma_\mu \gamma_5 \langle u_\nu F_{\alpha\beta}^- \rangle \Big\} \Psi \qquad . \qquad (2.31)
\end{aligned}
$$

where we have also shown the terms of dimension two since the form given in [19] is not minimal and can be reduced to the one shown here. We do not discuss the renormalization of this effective field theory since the power counting can not be set up in a straightforward way. A thorough and detailed discussion is given in ref. [19].

2.2 Effective Lagrangian in the heavy fermion limit

We are now in the position to perform the extreme non-relativistic limit, i.e. to construct the heavy baryon effective field theory. Our procedure follows closely the one in [17], therefore we only give some steps for completeness. Basically, one considers the mass of the nucleon large compared to the typical external momenta transferred by pions or photons and writes the nucleon four–momentum as

$$
p_\mu = m\, v_\mu + \ell_\mu \, , \quad p^2 = m^2 \, , \quad v \cdot \ell \ll m \, . \qquad (2.32)
$$

Notice that later we have to differentiate between m (the physical nucleon mass) and $\mathring{m}$ (the nucleon mass in the chiral limit) when we consider the nucleon mass shift and wave function renormalization. Here, v_μ is the nucleon four–velocity (in the rest–frame, we have $v_\mu = (1, \vec{0}\,)$). In that case, we can decompose the wavefunction $\Psi(x)$ into velocity eigenstates [21] [17]

$$\Psi(x) = \exp[-imv \cdot x]\,[H(x) + h(x)] \tag{2.33}$$

with

$$\not{v}\; H = H\;, \not{v}\; h = -h\;, \tag{2.34}$$

or in terms of velocity projection operators

$$P_v^+ H = H\,,\; P_v^- h = h\,, \quad P_v^\pm = \frac{1}{2}(1 \pm \not{v})\,, \quad P_v^+ + P_v^- = 1\,. \tag{2.35}$$

One now eliminates the 'small' component $h(x)$ either by using the equations of motion or path–integral methods. The Dirac equation for the velocity–dependent baryon field $H = H_v$ (we will always suppress the label 'v') takes the form $iv \cdot \partial H_v = 0$ to lowest order in $1/m$. This allows for a consistent chiral counting as described and the effective pion–nucleon Lagrangian takes the form:[#9]

$$\mathcal{L}_{\pi N}^{(1)} = \bar{H}\,(iv \cdot D + g_A S \cdot u)\,H + \mathcal{O}\left(\frac{1}{m}\right)\,, \tag{2.36}$$

with S_μ the covariant spin–operator

$$S_\mu = \frac{i}{2}\gamma_5 \sigma_{\mu\nu} v^\nu\,,\; S \cdot v = 0\,,\; \{S_\mu, S_\nu\} = \frac{1}{2}\,(v_\mu v_\nu - g_{\mu\nu})\;,\; [S_\mu, S_\nu] = i\epsilon_{\mu\nu\gamma\delta} v^\gamma S^\delta\;, \tag{2.37}$$

in the convention $\epsilon^{0123} = -1$. There is one subtlety to be discussed here. In the calculation of loop graphs, divergences appear which need to be regularized and renormalized. This is most easily done in dimensional regularization since it naturally preserves the underlying symmetries. However, the totally antisymmetric Levi-Civita tensor is ill-defined in $d \neq 4$ space–time dimensions. One therefore has to be careful with the spin algebra. In essence, one has to give a prescription to uniquely fix the finite pieces. The mostly used convention is to only use the anticommutator to simplify products of spin matrices and solely take into account that the commutator is antisymmetric under interchange of the indices. Furthermore, S^2 can be uniquely extended to d dimensions via $S^2 = (1-d)/4$. With that in mind, two important observations can be made: Eq.(2.36) does not contain the nucleon mass term any more and also, all Dirac matrices can be expressed as combinations of v_μ and S_μ. With these rules, which are given for completeness in appendix B, we can translate all terms of the relativistic Lagrangian, Eq.(2.31), into their heavy fermion counterpieces. These terms are accompanied by LECs, which we call d_i, $i = 1, \ldots, 23$.

[#9] Note that the parameters appearing in the effective Lagrangian should be taken at their values in the chiral limit.

In addition, there are $1/m$ corrections to the various operators. These can be worked out along the lines spelled out in appendix A of ref.[17]. As an example, consider the part of the third order action which has the form

$$S'_{\pi N} = -\frac{1}{(2m)^2} \int d^4x \, \bar{H} \, (\gamma_0 \, \mathcal{B}^{(1)\dagger} \, \gamma_0)(iv \cdot D + g_A S \cdot u) \, \mathcal{B}^{(1)} \, H \ , \tag{2.38}$$

which translates into the following piece of the third order effective Lagrangian,

$$\mathcal{L}^{(3)'}_{\pi N} = -\frac{1}{4m^2} \bar{H} \left[(i \not{D}^\perp + \frac{1}{2} g_A v \cdot u \gamma_5)(iv \cdot D + g_A S \cdot u)(i \not{D}^\perp - \frac{1}{2} g_A v \cdot u \gamma_5) \right] H \ , \tag{2.39}$$

with $D^\perp_\mu = (g_{\mu\nu} - v_\mu v_\nu) D^\nu$. One now has to express the various products of derivatives, γ matrices and so on, in terms of non–relativistic four–vectors. For the product of the first terms in the three square brackets, this amounts to

$$\bar{H} \not{D}^\perp \, v \cdot D \not{D}^\perp \, H = \bar{H} [(v \cdot D)^3 + D_\mu v \cdot D D^\mu - 2 [S_\mu, S_\nu] \, D^\mu v \cdot D D^\nu] H \ , \tag{2.40}$$

so that

$$\mathcal{L}^{(3)'}_{\pi N} = -\frac{i}{4m^2} \bar{H} \left[(v \cdot D)^3 - D_\mu v \cdot D D^\mu + 2 [S_\mu, S_\nu] D^\mu v \cdot D D^\nu + \ldots \right] H \ . \tag{2.41}$$

With 8 other relations of this type one can fill in the ellipsis. Similarly, the other pieces contributing at this order can be worked out.

Finally, one has to renormalize the one–loop generating functional. This can be done along the lines described in [22] and detailed in [23]. All divergences can be absorbed in the LECs of the 23 terms previously constructed. In fact, only 14 of these are divergent. For these, we introduce scale–dependent renormalized values,

$$d_i = d_i^r(\lambda) + \frac{\kappa_i}{(4\pi F)^2} \, \mathrm{L}(\lambda) \ , \tag{2.42}$$

with

$$\mathrm{L}(\lambda) = \frac{\lambda^{d-4}}{16\pi^2} \left\{ \frac{1}{d-4} - \frac{1}{2} \left[\ln(4\pi) + \Gamma'(1) + 1 \right] \right\} \quad , \tag{2.43}$$

and λ is the scale of dimensional regularization. In addition, there are eigth terms which are only necessary for the renormalization, i.e. that do not appear in matrix elements of physical processes. To be precise, these terms stem solely from the divergent part of the one–loop generating functional and have no (finite) counterparts in the relativistic theory. Note also that all these terms are proportional to the nucleon eom, $v \cdot D \, H$, and thus can be transformed away by appropriate field redefinitions.

Putting pieces together, the complete third order Lagrangian takes the form

$$\begin{aligned} \mathcal{L}^{(3)}_{\pi N} &= \mathcal{L}^{(3),\,\mathrm{fixed}}_{\pi N} + \sum_{i=1}^{23} d_i \, \bar{H} \tilde{O}_i H + \sum_{i=24}^{31} \tilde{d}_i \, \bar{H} \tilde{O}_i^{\mathrm{div}} H \ , \\ &= \bar{H} \left\{ \mathcal{O}^{(3)}_{\mathrm{fixed}} + \mathcal{O}^{(3)}_{\mathrm{ct}} + \mathcal{O}^{(3)}_{\mathrm{div}} \right\} H \ , \end{aligned} \tag{2.44}$$

with

$$
\begin{aligned}
\mathcal{O}^{(3)}_{\rm fixed} &= \frac{g_A}{8m^2}\,[D^\mu,[D_\mu,S\cdot u]] - \frac{g_A^2}{32m^2}\,\epsilon^{\mu\nu\alpha\beta}v_\alpha S_\beta\langle F^-_{\mu\nu}v\cdot u\rangle - i\,\frac{1}{4m^2}\,(v\cdot D)^3 \\
&- \frac{g_A}{4m^2}\,v\cdot\overleftarrow{D}\;S\cdot u\,v\cdot D + \frac{1}{8m^2}\left(i\,D^2\,v\cdot D + \text{h.c.}\right) \\
&- \frac{g_A}{4m^2}\,(\{S\cdot D, v\cdot u\}\,v\cdot D + \text{h.c.}) + \frac{3g_A^2}{64m^2}\left(i\langle(v\cdot u)^2\rangle\,v\cdot D + \text{h.c.}\right) \\
&+ \frac{1}{32m^2}\left(\epsilon^{\mu\nu\alpha\beta}v_\alpha S_\beta[u_\mu,u_\nu]\,v\cdot D + \text{h.c.}\right) \\
&- \frac{1}{16m^2}\left(i\,\epsilon^{\mu\nu\alpha\beta}v_\alpha S_\beta\hat{F}^+_{\mu\nu}v\cdot D + \text{h.c.}\right) \\
&- \frac{g_A}{8m^2}\left(S\cdot u\,D^2 + \text{h.c.}\right) - \frac{g_A}{4m^2}\left(S\cdot\overleftarrow{D}\;u\cdot D + \text{h.c.}\right) \\
&- \frac{1+2c_6}{8m^2}\,\left(i\,\epsilon^{\mu\nu\alpha\beta}v_\alpha S_\beta\hat{F}^+_{\mu\sigma}v^\sigma D_\nu + \text{h.c.}\right) \\
&- \frac{c_7}{4m^2}\left(i\,\epsilon^{\mu\nu\alpha\beta}v_\alpha S_\beta\langle F^+_{\mu\sigma}\rangle\,v^\sigma D_\nu + \text{h.c.}\right) \\
&+ \frac{1+g_A^2+8m\,c_4}{16m^2}\left(\epsilon^{\mu\nu\alpha\beta}v_\alpha S_\beta[u_\mu,v\cdot u]D_\nu + \text{h.c.}\right) \\
&+ \frac{g_A}{32m^2}\left(i\,\epsilon^{\mu\nu\alpha\beta}v_\alpha F^-_{\mu\nu}D_\beta + \text{h.c.}\right) - \frac{g_A^2}{16m^2}\,(i\,v\cdot u\,u\cdot D + \text{h.c.}) \\
&+ i\,\frac{1+8m\,c_4}{32m^2}\,[v\cdot u,[D^\mu,u_\mu]] + \frac{c_2}{2m}\,(i\langle v\cdot u\,u_\mu\rangle D^\mu + \text{h.c.})\ , \qquad (2.45)
\end{aligned}
$$

$$
\begin{aligned}
\mathcal{O}^{(3)}_{\rm ct} &= i\,d_1(\lambda)\,[u_\mu,[v\cdot D,u^\mu]] + i\left(d_2(\lambda) - \frac{1+8m\,c_4}{32m^2}\right)[u_\mu,[D^\mu,v\cdot u]] \\
&+ i\left(d_3(\lambda) + \frac{g_A^2}{32m^2}\right)[v\cdot u,[v\cdot D,v\cdot u]] \\
&+ i\left(d_4(\lambda) - \frac{g_A}{64m^2}\right)\epsilon^{\mu\nu\alpha\beta}v_\alpha\langle u_\mu u_\nu u_\beta\rangle + d_5(\lambda)\,[\chi_-,v\cdot u] \\
&+ \left(d_6(\lambda) - \frac{1+2c_6}{16m^2}\right)[D^\mu,\hat{F}^+_{\mu\nu}]\,v^\nu + \left(d_7 - \frac{c_7}{8m^2}\right)[D^\mu,\langle F^+_{\mu\nu}\rangle]\,v^\nu \\
&+ \left(d_8(\lambda) + \frac{g_A}{64m^2}\right)\epsilon^{\mu\nu\alpha\beta}v_\beta\langle\hat{F}^+_{\mu\nu}u_\alpha\rangle \\
&+ \left(d_9 + \frac{g_A}{64m^2}\right)\epsilon^{\mu\nu\alpha\beta}v_\beta\langle F^+_{\mu\nu}\rangle\,u_\alpha + d_{10}(\lambda)\,S\cdot u\,\langle u\cdot u\rangle
\end{aligned}
$$

$$
\begin{aligned}
&+ \quad d_{11}(\lambda)\, S^\mu u^\nu \langle u_\mu u_\nu \rangle \\
&+ \quad \left(d_{12}(\lambda) - \frac{4 g_A (1 + 4m\, c_4) + g_A^3}{32 m^2} \right) S\cdot u\, \langle (v\cdot u)^2 \rangle \\
&+ \quad \left(d_{13}(\lambda) + \frac{2 g_A (1 + 4m\, c_4) + g_A^3}{16 m^2} \right) S^\mu v\cdot u\, \langle u_\mu v\cdot u \rangle \\
&+ \quad d_{14}(\lambda)\, \epsilon^{\mu\nu\alpha\beta} v_\alpha S_\beta \langle [v\cdot D, u_\mu]\, u_\nu \rangle \\
&+ \quad \left(d_{15} + \frac{g_A^2}{16 m^2} \right) \epsilon^{\mu\nu\alpha\beta} v_\alpha S_\beta \langle u_\mu [D_\nu, v\cdot u] \rangle \\
&+ \quad d_{16}(\lambda)\, S\cdot u\, \langle \chi_+ \rangle + d_{17}\, S^\mu \langle u_\mu \chi_+ \rangle + i\, d_{18}\, S^\mu [D_\mu, \chi_-] \\
&+ \quad i\, d_{19}\, S^\mu [D_\mu, \langle \chi_- \rangle] + i \left(d_{20}(\lambda) + \frac{g_A (1 - c_6)}{8 m^2} \right) S^\mu v^\nu [\hat{F}^+_{\mu\nu}, v\cdot u] \\
&+ \quad i\, d_{21}\, S^\mu [\hat{F}^+_{\mu\nu}, u^\nu] + d_{22}\, S^\mu [D^\nu, F^-_{\mu\nu}] + d_{23}\, \epsilon^{\mu\nu\alpha\beta} S_\mu \langle u_\nu F^-_{\alpha\beta} \rangle \ , \qquad (2.46)
\end{aligned}
$$

$$
\begin{aligned}
\mathcal{O}^{(3)}_{\rm div} \ &= \ \tilde{d}_{24}(\lambda)\, i\, (v\cdot D)^3 + \tilde{d}_{25}(\lambda)\, v\cdot \overleftarrow{D}\, S\cdot u\, v\cdot D + \tilde{d}_{26}(\lambda)\, (i\, \langle u\cdot u \rangle\, v\cdot D + \text{h.c.}) \\
&+ \quad \tilde{d}_{27}(\lambda) \left(i\, \langle (v\cdot u)^2 \rangle\, v\cdot D + \text{h.c.} \right) + \tilde{d}_{28}(\lambda)\, (i\, \langle \chi_+ \rangle\, v\cdot D + \text{h.c.}) \\
&+ \quad \tilde{d}_{29}(\lambda)\, (S^\mu [v\cdot D, u_\mu]\, v\cdot D + \text{h.c.}) \\
&+ \quad \tilde{d}_{30}(\lambda) \left(\epsilon^{\mu\nu\alpha\beta} v_\alpha S_\beta [u_\mu, u_\nu]\, v\cdot D + \text{h.c.} \right) \\
&+ \quad \tilde{d}_{31}(\lambda) \left(\epsilon^{\mu\nu\alpha\beta} v_\alpha S_\beta \hat{F}^+_{\mu\nu}\, v\cdot D + \text{h.c.} \right) \ . \qquad (2.47)
\end{aligned}
$$

Note that for the counterterms, one can also introduce scale–independent LECs $\bar{d}_i$ via

$$
d_i(\lambda) = \bar{d}_i + \frac{\kappa_i}{(4\pi F)^2} \left((4\pi)^2\, \mathrm{L} - \log \frac{\lambda}{M} \right) \ , \qquad (2.48)
$$

and the LECs for the operators needed for the renormalization only have, of course, no finite piece,

$$
\tilde{d}_i(\lambda) = \frac{\tilde{\kappa}_i}{(4\pi F)^2} \left((4\pi)^2\, \mathrm{L} - \log \frac{\lambda}{M} \right) \ . \qquad (2.49)
$$

Note that in ref.[13] this Lagrangian was first given in another basis. In that paper, however, there is one term too much (their operator O_4 has a fixed coefficient c_2/m). The form of the effective pion–nucleon Lagrangian given here is most convenient for direct comparison with the many calculations done in the basis of the review [17]. The novel Feynman rules from the dimension three Lagrangian relevant for the problem of pion–nucleon scattering are collected in app. C. For an easier comparison with the Lagrangian

given in [13], we have ordered the operators in the same way. This means that their b_i can be mapped on our d_i for $i = 1, 2, 3$ and their b_{i+1} onto d_i for $i = 4, \ldots, 23$. Note that the b_i also contain some finite pieces which are separated out explicitely in our dimension three Lagrangian. We refer the reader to [20] for a more detailed comparison. The β functions κ_i and $\tilde{\kappa}_i$ can be inferred from ref.[22]. For completeness, we list them here for our basis:

$$\begin{aligned}
\kappa_1 &= g_A^4/8\ ,\ \kappa_2 = -(1+5g_A^2)/12\ ,\ \kappa_3 = (4-g_A^4)/8\ ,\ \kappa_4 = -g_A^3(4+3g_A^2)/16\ , \\
\kappa_5 &= (1+5g_A^2)/24\ ,\ \kappa_6 = -(1+5g_A^2)/6\ ,\ \kappa_8 = g_A^3/4\ ,\ \kappa_{10} = g_A(4-g_A^4)/8\ , \\
\kappa_{11} &= g_A(6-6g_A^2+g_A^4)/12\ ,\ \kappa_{12} = -g_A(8-g_A^4)/8\ ,\ \kappa_{13} = -g_A^5/12\ , \\
\kappa_{14} &= -g_A^4/4\ ,\ \kappa_{16} = g_A(4-g_A^2)/8\ ,\ \kappa_{20} = g_A\ , \\
\tilde{\kappa}_{24} &= -3g_A^2\ ,\ \tilde{\kappa}_{25} = g_A^3\ ,\ \tilde{\kappa}_{26} = -3g_A^2(4+3g_A^2)/16\ ,\ \tilde{\kappa}_{27} = (8+9g_A^4)/16\ , \\
\tilde{\kappa}_{28} &= -9g_A^2/16\ ,\ \tilde{\kappa}_{29} = g_A^3/3\ ,\ \tilde{\kappa}_{30} = -g_A^2(4+g_A^2)/8\ ,\ \tilde{\kappa}_{31} = g_A^2\ . \qquad (2.50)
\end{aligned}$$

Having constructed the effective pion–nucleon Lagrangian to order q^3, we now turn to apply it to elastic pion–nucleon scattering. To account for isospin breaking, one also has to extend this Lagrangain to include virtual photons. This has already been done in [16] and we refer the reader to that paper. For a systematic study of isospin violation in the elastic and charge exchange channels, one first has to find out to what accuracy the low energy πN phase shifts can be described in the isospin symmetric framework. This is the question which will be addressed in the remaining sections of this investigation.

3 Pion–nucleon scattering

3.1 Basic definitions

In the following, we consider the πN-scattering amplitude. In the center-of-mass system (cms) the amplitude for the process $\pi^a(q_1) + N(p_1) \to \pi^b(q_2) + N(p_2)$ takes the following form (in the isospin basis):

$$\begin{aligned}
T_{\pi N}^{ba} &= \left(\frac{E+m}{2m}\right)\Big\{\delta^{ba}\Big[g^+(\omega,t) + i\vec{\sigma}\cdot(\vec{q}_2\times\vec{q}_1\,)\,h^+(\omega,t)\Big] \\
&\qquad + i\,\epsilon^{bac}\tau^c\Big[g^-(\omega,t) + i\vec{\sigma}\cdot(\vec{q}_2\times\vec{q}_1\,)\,h^-(\omega,t)\Big]\Big\} \qquad (3.1)
\end{aligned}$$

with $\omega = v\cdot q_1 = v\cdot q_2$ the pion cms energy, $t = (q_1-q_2)^2$ the invariant momentum transfer squared, $E_1 = E_2 \equiv E = (\vec{q}^{\,2}+m^2)^{1/2}$ the nucleon energy and

$$\vec{q}_1^{\,2} = \vec{q}_2^{\,2} \equiv \vec{q}^{\,2} = \frac{(s-M^2-m^2)^2 - 4m^2M^2}{4s} \quad . \qquad (3.2)$$

Furthermore, $g^\pm(\omega,t)$ refers to the isoscalar/isovector non-spin-flip amplitude and $h^\pm(\omega,t)$ to the isoscalar/isovector spin-flip amplitude. This form is most suitable for the HBCHPT

calculation since it is already defined in a two–component framework.[#10] A more detailed discussion of the pertinent kinematical relations (also for the case of different nucleon and pion masses in the in– and out–going states) is given in app. D. We note that Mojžiš [12] has introduced two–component amplitudes $\alpha^\pm$ and $\beta^\pm$ which are related to the ones we use via[#11]

$$g^\pm = \alpha^\pm \ , \quad h^\pm = -\frac{1}{2}\beta^\pm \ . \tag{3.3}$$

The difference in the spin–flip amplitude is due to our use of the Pauli matrices whereas in [12] the spin–vector S_μ was used. The partial wave amplitudes $f^\pm_{l\pm}(s)$, where l refers to the orbital angular momentum, the superscript '$\pm$' to the isospin and the subscript '$\pm$' to the total angular momentum ($j = l \pm s$), are given in terms of the invariant amplitudes via

$$f^\pm_{l\pm}(s) = \frac{E+m}{16\pi\sqrt{s}} \int_{-1}^{+1} dz \left[g^\pm \, P_l(z) + \vec{q}^{\,2} \, h^\pm \left(P_{l\pm1}(z) - z P_l(z) \right) \right] , \tag{3.4}$$

where $z = \cos(\theta)$ is the angular variable and $\sqrt{s}$ the total cms energy. The $P_l(z)$ are the conventional Legendre polynoms. For a given isospin I, the phase shifts $\delta^I_{l\pm}(s)$ can be extracted from the partial waves via

$$f^I_{l\pm}(s) = \frac{1}{2i|\vec{q}\,|} \left[\exp(2i\delta^I_{l\pm}) - 1 \right] . \tag{3.5}$$

For vanishing inelasticity, which is the case for the energy range considered in this work, the phase shifts are real. They are given by (for a detailed discussion about the issue of defining the phase shifts in an effective field theory, see ref.[24])

$$\delta^I_{l\pm}(s) = \arctan(|\vec{q}\,| \, \mathrm{Re} \ f^I_{l\pm}(s)) \ . \tag{3.6}$$

Equally well, one could use the definition without the arctan, the difference being of higher order. For the phase shifts in the kinematical region considered below, this difference is negligible.

What we are after is the chiral expansion of the various amplitudes $g^\pm, h^\pm$. These consist of essentially three pieces, which are the Born and counterterm parts of polynomial type as well as the unitarity corrections due to the pion loops. To be precise, we have

$$X = X^{\rm tree} + X^{\rm ct} + X^{\rm loop} \ , \quad X = g^\pm, h^\pm \ , \tag{3.7}$$

where the tree contribution subsumes all terms generated from the lowest order Lagrangian, the counter term amplitude the ones proportional to the dimension two and three LECs (i.e. $\sim c_i, c_i/m, d_i$) and the last term in Eq.(3.7) is the one–loop order q^3 amplitude. The latter is a complex–valued function and restores unitarity in the perturbative sense. Its various terms are all proportional to $1/F^4$. These amplitudes are functions of two kinematical variables. We choose the pion energy and the invariant momentum transfer squared, i.e. $X = X(\omega, t)$. In what follows, we mostly suppress these arguments. Before discussing the full order q^3 one–loop amplitude, we wish to elaborate on the relativistic tree graphs with insertions from the dimension one effective Lagrangian. These terms are all proportional to g_A^2/F^2 or $1/F^2$.

[#10] These amplitudes should not be called "non-relativistic". They are, however, more suitable for our discussion than the amplitudes $A^\pm(s,t), B^\pm(s,t)$ which arise from a manifest Lorentz–invariant formulation of the πN scattering amplitude.

[#11] Note, however, that in [12] the amplitudes are evaluated in a particular frame, which is not the cms. Therefore, care has to be taken when comparing our amplitudes with the ones of Mojžiš.

3.2 Evaluation of the tree graphs

In this section we wish to elaborate on the tree amplitudes $X^{\rm tree}$. It was already stated in [25] that the most convenient way to calculate the chiral expansion of these is to take the relativistic theory and expand the resulting amplitudes in powers of $1/m$ to the order one is working. Ecker and Mojžiš [26] have given a different prescription for calculating in the heavy fermion formalism. Their procedure involves an unusual, momentum–dependent wavefunction renormalization. We show here that one can indeed recover the relativistic result from the heavy fermion theory by straightforward calculation to third order and for the process under consideration. A general proof of the equivalence between this method and the one proposed in [26] is given in ref.[44]

Consider first the relativistic tree graphs shown in fig. 1. These are the nucleon pole graph (fig. 1a), its crossed partner (fig. 1b) and the seagull term (fig. 1c) involving the non–linear pion–nucleon $\bar{N}N\pi\pi$ vertex. Using the notation of app. D, their respective contributions are

$$\begin{aligned}
T_{\pi N}^{(a)} &= \frac{g_A^2}{4F^2}\,\tau^b\tau^a\,\bar{u}(p_2)\;\not{q}_2\;\frac{-\not{p}_1-\not{q}_1+m}{(p_1+q_1)^2-m^2}\;\not{q}_1\;u(p_1)\;,\\
T_{\pi N}^{(b)} &= \frac{g_A^2}{4F^2}\,\tau^a\tau^b\,\bar{u}(p_2)\;\not{q}_1\;\frac{-\not{p}_1+\not{q}_2+m}{(p_1-q_2)^2-m^2}\;\not{q}_2\;u(p_1)\;,\\
T_{\pi N}^{(c)} &= -\frac{i}{4F^2}\,\epsilon^{abc}\tau^c\,\bar{u}(p_2)\,(\not{q}_1+\not{q}_2)\,u(p_1)\;. \qquad (3.8)
\end{aligned}$$

Note that while the first two terms have an isoscalar and an isovector contribution, the seagull term is purely isovector. It is also important to remember that all quantities appearing in these formulas, such as the nucleon mass, the axial-vector coupling etc., are taken at their chiral limit values. For a more compact notation, we refrain from denoting these by the symbol '$\circ$'. The nucleon spinors are normalized as given in Eq.(D.9) and we will not expand these normalization factors in what follows. Straightforward algebra allows one to extract the amplitudes $g^\pm, h^\pm$ from these expressions. Putting all pieces together and expanding up–to–and–including order $1/m^2$, we find

$$\begin{aligned}
g^+(\omega,t) &= -\frac{g_A^2}{F^2}\frac{1}{16m\omega^2}\Big[4M^4+t^2+4\omega^2t-4M^2t\Big]\\
&+\frac{g_A^2}{F^2}\frac{1}{32m^2\omega^3}\Big[16\omega^2M^4+5\omega^2t^2-16M^6-8M^2t^2+4\omega^4t+20M^4t\\
&\qquad +t^3-20\omega^2M^2t\Big]\;, \qquad (3.9)\\
g^-(\omega,t) &= -\frac{g_A^2}{F^2}\frac{1}{4\omega}\Big[2\omega^2-2M^2+t\Big]+\frac{\omega}{2F^2}\\
&+\frac{g_A^2}{F^2}\frac{1}{16m\omega^2}\Big[t^2+2\omega^2t-8\omega^4+8M^4-6M^2t\Big]-\frac{1}{8mF^2}\Big[4M^2-4\omega^2-t\Big]\\
&+\frac{g_A^2}{F^2}\frac{1}{32m^2\omega^3}\Big[8M^2\omega^4-20M^4\omega^2-4\omega^6+20M^6+20\omega^2M^2t-5\omega^2t^2-4t\omega^4
\end{aligned}$$

$$-22M^4t+8t^2M^2-t^3\Big]+\frac{\omega}{16m^2F^2}\Big[2\omega^2-2M^2+t\Big]\,, \qquad (3.10)$$

$$\begin{aligned} h^+(\omega,t) &= -\frac{g_A^2}{F^2}\frac{1}{2\omega}-\frac{g_A^2}{F^2}\frac{1}{8m\omega^2}\Big[4M^2-t\Big] \\ &- \frac{g_A^2}{F^2}\frac{1}{16m^2\omega^3}\Big[10M^4+t^2-6\omega^2M^2-2\omega^4+3t\omega^2-6M^2t\Big]\,, \qquad (3.11) \\ h^-(\omega,t) &= -\frac{g_A^2}{F^2}\frac{1}{8m\omega^2}\Big[2\omega^2-2M^2+t\Big]+\frac{1}{F^2}\frac{1}{4m} \\ &- \frac{g_A^2}{F^2}\frac{1}{16m^2\omega^3}\Big[2\omega^4-t^2-8M^4+6M^2t-3\omega^2t+6\omega^2M^2\Big]+\frac{\omega}{8m^2F^2}\,. \qquad (3.12) \end{aligned}$$

Consider now the equivalent graphs in the heavy fermion language. They are shown in fig. 2. The heavy dot (box) denotes a dimension two (three) insertion with a *fixed* coefficient, i.e. all LECs are set to zero (they contribute to $X^{\rm ct}$). Using the Feynman rules of app. C, one can work out these diagrams straightforwardly. We stress that we take the same normalization factor as for the relativistic calculation, which again is not expanded. This is different from the treatment in ref. [12]. We give here only some illustrative intermediate results. The T–matrix corresponding to diagrams 1a,2a, and 3a reads:

$$\begin{aligned} T_{\pi N}^{(1a)} &= -\mathcal{N}^2\frac{g_A^2}{F^2}\,\tau^b\tau^a\,S\cdot q_2\,S\cdot q_1\,\frac{1}{v\cdot(p_1+q_1)}\,, \\ T_{\pi N}^{(2a)} &= \mathcal{N}^2\frac{g_A^2}{F^2}\,\frac{1}{2m}\,\tau^b\tau^a\,S\cdot q_2\,S\cdot(2p_2+2q_2-q_1)\frac{v\cdot q_1}{v\cdot(p_1+q_1)}\,, \\ T_{\pi N}^{(3a)} &= \mathcal{N}^2\frac{g_A^2}{F^2}\,\frac{1}{8m^2}\,\tau^b\tau^a\,\frac{1}{v\cdot(p_1+q_1)}\,S\cdot q_2\,S\cdot q_1 \\ &\times\ 2\Big[v\cdot p_1\,v\cdot(p_1+q_1)-(p_1+q_1)^2+v\cdot(2p_1+q_1)v\cdot q_1\Big]\,, \qquad (3.13) \end{aligned}$$

with $\mathcal{N}$ defined in Eq.(D.9) (here for the equal mass case). Dissecting these into spin–dependent and independent terms, we get (including also the crossed diagrams) as contributions to the invariant amplitudes in the cms:

$$\begin{aligned} g_{(1a)}^{\pm} &= -\frac{g_A^2}{F^2}\frac{1}{8}(2\omega^2-2M^2+t)\left[\frac{1}{v\cdot(p_1+q_1)}\pm\frac{1}{v\cdot(p_1-q_2)}\right]\,, \qquad (3.14) \\ h_{(1a)}^{\pm} &= \frac{g_A^2}{F^2}\frac{1}{4}\Big[\frac{-1}{v\cdot(p_1+q_1)}\pm\frac{1}{v\cdot(p_1-q_2)}\Big]\,, \qquad (3.15) \\ g_{(2a)}^{\pm} &= \frac{g_A^2}{F^2}\frac{1}{2m}\Big[-\frac{1}{8}(2\omega^2-2M^2+t)\frac{v\cdot q_1}{v\cdot(p_1+q_1)} \\ &\qquad \pm\Big(2S\cdot q_1 S\cdot p_1-\frac{1}{8}(2\omega^2-2M^2+t)\Big)\frac{v\cdot q_2}{v\cdot(p_1-q_2)}\Big]\,, \qquad (3.16) \\ h_{(2a)}^{\pm} &= -\frac{g_A^2}{F^2}\frac{1}{8m}\Big[\frac{v\cdot q_1}{v\cdot(p_1+q_1)}\mp\frac{v\cdot q_2}{v\cdot(p_1-q_2)}\Big]\,, \qquad (3.17) \end{aligned}$$

$$
\begin{aligned}
g^{\pm}_{(3a)} &= \frac{g_A^2}{F^2}\frac{1}{8m^2}\Big\{\frac{1}{8}(2\omega^2-2M^2+t)\Big[\frac{1}{v\cdot(p_1+q_1)}(q_1^2+2v\cdot p_1 v\cdot(p_1+q_1)\\
&- (p_1+q_1)^2-p_1^2+2v\cdot(2p_1+q_1)v\cdot q_1-2q_1\cdot(p_1+q_1))\\
&\pm \frac{1}{v\cdot(p_1-q_2)}(q_2^2+2v\cdot p_1 v\cdot(p_1-q_2)-(p_1-q_2)^2-p_1^2\\
&+ 2v\cdot(2p_1-q_2)v\cdot q_2-2q_2\cdot p_1)\Big]\pm\frac{1}{2}\frac{\omega_1^2-q_1^2}{v\cdot(p_1-q_2)}\times\\
&\qquad\qquad\Big[2v\cdot(2p_1-q_2)v\cdot q_2-q_2\cdot(2p_1-q_2)\Big]\Big\}\,, \qquad (3.18)\\
h^{\pm}_{(3a)} &= \frac{g_A^2}{F^2}\frac{1}{32m^2}\Big\{\frac{1}{v\cdot(p_1+q_1)}(q_1^2+2v\cdot p_1 v\cdot(p_1+q_1)-(p_1+q_1)^2-p_1^2\\
&\qquad +2v\cdot(2p_1+q_1)v\cdot q_1-2q_1\cdot(p_1+q_1))\\
&\mp \frac{1}{v\cdot(p_1-q_2)}(q_2^2+2v\cdot p_1 v\cdot(p_1-q_2)-(p_1-q_2)^2-p_1^2\\
&\qquad +2v\cdot(2p_1-q_2)v\cdot q_2-2q_2\cdot p_1)\Big\}\,. \qquad (3.19)
\end{aligned}
$$

The other diagrams shown in fig. 2 can be evaluated similarly. Putting all pieces together, one *exactly* recovers the amplitude calculated by expanding the relativistic tree graphs, cf. Eq.(3.9-3.12). We are presently investigating other observables like the electromagnetic form factors and so on to show that this method can be employed in any situation. This is indeed proven in ref.[44].

3.3 One loop result for the amplitudes

The full one–loop amplitude to order q^3 is obtained after mass and coupling constant renormalization,

$$
(\mathring{g}_A, \mathring{m}, F, M) \to (g_A, m, F_\pi, M_\pi)\ . \qquad (3.20)
$$

The pertinent formulas can be found in refs. [6, 27]. The tree level amplitudes are given by the expressions of Eqs.(3.9-3.12), with the important difference that all parameters are taken at their *physical* values, not the ones in the chiral limit. For the construction of the loop and the counterterm amplitudes, we use the scale–independent LECs $\bar{d}_i$, so that in our final expressions all terms $\sim \ln(M_\pi/\lambda)$ have disappeared. Nevertheless, our amplitude agrees with the one given in appendix A of [11]. We have:

$$
\begin{aligned}
g^{+}_{\rm ct} &= \frac{1}{F^2}\Big[-4c_1M^2+2c_2\omega^2+c_3(2M^2-t)\Big]+\frac{c_2\,\omega}{mF^2}\Big[4\omega^2-4M^2+t\Big]\,, \qquad (3.21)\\
g^{+}_{\rm loop} &= i\,\frac{\omega^2}{8\pi F^4}\sqrt{\omega^2-M^2}+\frac{g_A^2}{F^4}\frac{1}{32\pi}\Big(M^2-2t\Big)\Big(M+\frac{2M^2-t}{2\sqrt{-t}}\arctan\frac{\sqrt{-t}}{2M}\Big)\\
&\qquad +\frac{g_A^4}{F^4}\frac{1}{24\pi\omega^2}\Big(t-2M^2+2\omega^2\Big)\Big[i(\omega^2-M^2)^{3/2}-M^3\Big]\,, \qquad (3.22)\\
g^{-}_{\rm ct} &= \frac{c_4\,\omega\,t}{2mF^2}+\frac{2\omega}{F^2}(2M^2-t)\,(\bar{d}_1+\bar{d}_2)+\frac{4\omega^3}{F^2}\,\bar{d}_3+\frac{8\omega\,M^2}{F^2}\,\bar{d}_5
\end{aligned}
$$

$$+\frac{g_A}{F^2}\frac{M^2}{\omega}(2\omega^2-2M^2+t)\,\bar{d}_{18}\ , \tag{3.23}$$

$$\begin{aligned} g^-_{\rm loop} &= \frac{1}{32\pi^2F^4}\Big\{\frac{\omega}{3}(4M^2-t)\sqrt{1-\frac{4M^2}{t}}\ln\frac{\sqrt{4M^2-t}+\sqrt{-t}}{2M} \\ &-4\omega^2\sqrt{\omega^2-M^2}\Big[-i\frac{\pi}{2}+\ln\Big(\frac{\omega}{M}+\sqrt{\frac{\omega^2}{M^2}-1}\Big)\Big]+\frac{\omega}{9}\Big(18\omega^2-12M^2+\frac{5}{2}t\Big)\Big\} \\ &+\frac{g_A^2}{24\pi^2F^4}\frac{1}{\omega}\Big\{-\frac{1}{4}\omega^2(5t-8M^2)\sqrt{1-\frac{4M^2}{t}}\ln\frac{\sqrt{4M^2-t}+\sqrt{-t}}{2M}-2\omega^2M^2+\frac{13}{24}\omega^2t\Big\} \\ &+\frac{g_A^4}{96\pi^2F^4}\frac{1}{\omega^2}(2M^2-2\omega^2-t)\Big\{-2(\omega^2-M^2)^{3/2}\Big[i\frac{\pi}{2}-\ln\Big(\frac{\omega}{M}+\sqrt{\frac{\omega^2}{M^2}-1}\Big)\Big] \\ &+2M^2\omega-\frac{5}{3}\omega^3\Big\}\ , \end{aligned} \tag{3.24}$$

$$h^+_{\rm ct} = \frac{2\omega}{F^2}\,(\bar{d}_{14}-\bar{d}_{15})+\frac{g_A}{F^2}\frac{2M^2}{\omega}\,\bar{d}_{18}\ , \tag{3.25}$$

$$h^+_{\rm loop} = -\frac{g_A^4}{24\pi^2F^4}\frac{1}{\omega^2}\Big\{M^2\omega+\frac{\omega^3}{6}-(\omega^2-M^2)^{3/2}\Big[i\frac{\pi}{2}-\ln\Big(\frac{\omega}{M}+\sqrt{\frac{\omega^2}{M^2}-1}\Big)\Big]\Big\}\ , \tag{3.26}$$

$$h^-_{\rm ct} = \frac{c_4}{F^2}+\frac{c_4\,\omega}{mF^2}\ , \tag{3.27}$$

$$h^-_{\rm loop} = \frac{g_A^2}{32\pi F^4}\Big[-M+\frac{t-4M^2}{2\sqrt{-t}}\arctan\frac{\sqrt{-t}}{2M}+\frac{4g_A^2}{3\omega^2}\Big(i(\omega^2-M^2)^{3/2}-M^3\Big)\Big]\ . \tag{3.28}$$

One can easily convince oneself that the imaginary parts stemming from the loop contributions at order q^3 fulfill perturbative unitarity. In terms of the partial wave amplitudes this reads:

$$\mathrm{Im}\ f_l^{I(3)}(s)=|\vec{q}_\pi\,|\Big(\mathrm{Re}\ f_l^{I(1)}(s)\Big)^2\ . \tag{3.29}$$

This is an important check of the calculation. The analytic structure of these amplitudes is further discussed in app. A of ref.[11]. Note also that the amplitudes have the proper crossing behaviour under $\omega_{\rm lab}\to-\omega_{\rm lab}$. In the formulas above, ω is given in the cms, but we remark that to the order we are working, $\omega_{\rm lab}=\omega_{\rm cms}$. More precisely, $\omega_{\rm lab}=\omega_{\rm cms}+(\omega^2_{\rm cms}-M^2)/m+$ higher orders.

4 Results

4.1 The fitting procedure

Before presenting the actual results, we have to discuss how to fix the four dimension two LECs and the five (combinations of) dimension three LECs. One way would be to fit to threshold and subthreshold parameters. Up to date, only the Karlsruhe (KA) analysis gives these consistently with the phase shifts [28]. From the point of the chiral expansion, this expansion around the center of the Mandelstam triangle together with the threshold parameters should provide the best data to fix the LECs. Since, however, some of the

data used in the KA analysis have become doubtful (for a detailed discussion see e.g. ref.[29]), we prefer to fit directly to the available six S– and P–wave phase shifts in a certain energy range, as discussed below. The threshold and subthreshold parameters are then predicted. We remark that there still is debate about the actual value of the isoscalar S–wave scattering length as extracted from pionic atoms [1] or the various partial–wave amplitudes. As input we use the phase shifts of the Karlsruhe (KA85) group [30], from the analysis of Matsinos [31] (EM98) and the latest update of the VPI group, called SP98 [32]. Since the Karlsruhe and the VPI groups give no errors for the phase shifts, we have assigned a common uncertainty of $\pm 3\%$ to all values. This procedure is, of course, somewhat arbitrary. We have convinced ourselves that assigning a different error to the phase shifts does not change the results but only the respective χ^2/dof. In case of the EM98 phases, we have used the given errors which vary for the various channels. Again, we find that the results are consistent with the ones for the other phases which gives us some confidence that our procedure is not quite useless. Preferrably, we would have worked with uncertainties provided directly by the various groups. This issue deserves further study. Note also that the LEC $\bar{d}_{18}$ is fixed by means of the Goldberger–Treiman discrepancy, i.e. by the value for the pion–nucleon coupling constant extracted in the various analyses,

$$g_{\pi N} = \frac{g_A\, m}{F_\pi}\Big(1 - \frac{2M_\pi^2\, \bar{d}_{18}}{g_A}\Big)\ . \tag{4.1}$$

The actual values of $g_{\pi N}$ are

$$g_{\pi N} = 13.4 \pm 0.1\,,\ \ 13.18 \pm 0.12\,,\ \ 13.13 \pm 0.03\,, \tag{4.2}$$

for KA85, EM98 and SP98. Throughout, we use $g_A = 1.26$, $F_\pi = 92.4\,\mathrm{MeV}$, $m = 938.27\,\mathrm{MeV}$ and $M_\pi = 139.57\,\mathrm{MeV}$. Finally, we remark that we do not use the value of the pion–nucleon σ–term in the fitting procedure. This would to a large extent determine the value of the LEC c_1. Due to the present discussion about the empirical value of the pion–nucleon σ–term [29], we prefer not to use it in the fit. We believe, however, that the analysis of [33] still gives the most trustworthy value for $\sigma_{\pi N}(0)$.

4.2 Phase shifts and threshold parameters

After the remarks of the preceeding paragraph, we can now present results. For the KA85 case, we have fitted the data up to 100 MeV pion lab momentum (i.e. 4 points per partial wave at $q_\pi = 40, 60, 79, 97$ MeV). For the analysis of Matsinos, we use 17 points for each partial wave in the range of $q_\pi = 41.4 - 96.3$ MeV for the fitting. For the VPI SP98 solution, one has all phases down to threshold. However, as pointed out to us by Pavan, the values at lower values of q_π are somewhat uncertain. Indeed, our fits underline this statement. Using only the values between threshold and $q_\pi = 50$ MeV, we are not able to get a low-χ^2 fit. If we use the 5 data points in the range between 60 and 100 MeV we get a stable fit. We also checked that extending the fitting range to higher energies, the fits become unstable due to the Delta resonance. From here on, we call the fits corresponding to the Karlsruhe, Matsinos and VPI analysis, fit 1, 2 and 3, in order. The resulting LECs are given in table 2. Note that the error on the LECs is purely the one given by the

LEC	Fit 1	Fit 2	Fit 3
c_1	-1.23 ± 0.16	-1.42 ± 0.03	-1.53 ± 0.18
c_2	3.28 ± 0.23	3.13 ± 0.04	3.22 ± 0.25
c_3	-5.94 ± 0.09	-5.85 ± 0.01	-6.20 ± 0.09
c_4	3.47 ± 0.05	3.50 ± 0.01	3.51 ± 0.04
$\bar{d}_1 + \bar{d}_2$	3.06 ± 0.21	3.31 ± 0.14	2.68 ± 0.15
$\bar{d}_3$	-3.27 ± 0.73	-2.75 ± 0.18	-3.11 ± 0.79
$\bar{d}_5$	0.45 ± 0.42	-0.48 ± 0.06	0.43 ± 0.49
$\bar{d}_{14} - \bar{d}_{15}$	-5.65 ± 0.41	-5.69 ± 0.28	-5.74 ± 0.29
$\bar{d}_{18}$	-1.40 ± 0.24	-0.78 ± 0.27	-0.83 ± 0.06

Table 2: Values of the LECs in GeV^{-1} and GeV^{-2} for the c_i and $\bar{d}_i$, respectively, for the various fits as described in the text.

fitting routine and is certainly underestimated. All the LECs come out of "natural size", i.e. they are numbers of order one. For that, one introduces the dimensionless LECs $c_i' = 2mc_i$ and $\bar{d}_i\,' = 4m^2\bar{d}_i$. Inspection of the values given above shows that all LECs turn out to be between one and ten (up to a sign, of course). A more detailed discussion of the values of these LECs is given in the next paragraph. The resulting S– and P–wave phase shifts are shown in figs. 3 (fit 1), 4 (fit 2) and 5 (fit 3). The corresponding χ^2/dof is 0.83, 0.77 and 1.34 for fits 1,2 and 3, respectively. Note, however, that only in the case of fit 2 this number is really meaningful since it reflects the uncertainties of the data as given in the analysis. The description of the phase shifts is surprisingly good even at higher energies and also for the P–waves. Even the bending of the P_{11} phase due to the Roper resonance can be reproduced in fit 3 but is clearly absent in fit 2. Furthermore, the tail of the Δ in the P_{33} channel is underestimated. Still, in an overall view these six lowest partial waves can be described fairly well in this $\mathcal{O}(q^3)$ calculation up to surprisingly large pion momenta.

Since we do not fit data below $q_\pi = 40, 41, 60\,\mathrm{MeV}$ (fit 1,2,3) , the threshold parameters are now predictions. These are shown for the various fits in table 3 in comparison to the empirical values of the various analyses. First, we observe that the numbers resulting from the one–loop calculation are consistent with the "empirical" ones. The latter are obtained by use of dispersion relations for KA85 and SP98[#12] and in the EM98 case with the help of a fairly precise tree level model [37]. One might, of course, question the validity of such an approach. Notice that the isoscalar S–wave scattering length can not be determined precisely within our calculation (as already noted in [8]) but we can give a range, $-1.0 \leq a_{0+}^+ \leq 0.6$ in units of $10^{-2}/M_{\pi^+}$. In this band falls also

[#12]To be precise, only the values for $a_{0+}^\pm$ and a_{1+}^+ are obtained by dispersion relations and the others by effective range fits for SP98. Some of the results based on the effective range fits appear to be "strange". We are grateful to Marcello Pavan for providing us with this information.

Obs.	Fit 1	Fit 2	Fit 3	KA85	EM98	SP98
a^+_{0+}	-0.97	0.49	0.25	-0.83	0.41 ± 0.09	0.0 ± 0.1
b^+_{0+}	-4.77	-5.23	-6.33	-4.40	-4.46	-4.83 ± 0.10
a^-_{0+}	9.05	7.72	8.72	9.17	7.73 ± 0.06	8.83 ± 0.07
b^-_{0+}	1.26	1.62	0.82	0.77	1.56	0.07 ± 0.07
a^+_{1-}	-5.52	-5.38	-4.90	-5.53	-5.46 ± 0.10	-5.33 ± 0.17
a^+_{1+}	13.97	13.66	14.21	13.27	13.13 ± 0.13	13.6 ± 0.1
a^-_{1-}	-1.36	-1.25	-0.98	-1.13	-1.19 ± 0.08	-1.00 ± 0.10
a^-_{1+}	-8.44	-8.40	-8.16	-8.13	-8.22 ± 0.07	-7.47 ± 0.13

Table 3: Values of the S– and P–wave threshold parameters for the various fits as described in the text in comparison to the respective data. Note that we have extracted $b^\pm_{0+}$ from the Matsinos phase shifts and thus no uncertainty is given. Units are appropriate inverse powers of the pion mass times 10^{-2}.

the recent HBCHPT determination based on the analysis of pion–deuteron scattering, $a^+_{0+} = (-0.30 \pm 0.05) \cdot 10^{-2}/M_{\pi^+}$ [34]. For the isovector S–wave scattering length, we find a more precise prediction:

$$8.3 \cdot 10^{-2}/M_{\pi^+} \leq a^-_{0+} \leq 9.3 \cdot 10^{-2}/M_{\pi^+} \ . \tag{4.3}$$

To arrive at this band, we have excluded the rather low value found for fit 2. This can be traced back to the fact that the third order LEC contribution $\sim M_\pi^3(\bar{d}_1 + \bar{d}_2 + \bar{d}_3 + 2\bar{d}_5)$, which is positive for fits 1,3 but is negative for fit 2 due to a negative value of $\bar{d}_5$ in that case. This band is consistent with the one given in [9]. In that paper, resonance saturation was used to estimate this particular combination of LECs. While one might question the accuracy of such an estimate, the sign should be given by the dominant Δ contribution which is positive for the off–shell parameter $Z < 0.5$. As discussed in the review [6], all phenomenological indications point towards a value of Z well below this limit. To arrive at the lower end of the range given in Eq.(4.3), we have set the third order counterterm contribution to zero. Finally, we remark that due to the large uncertainty in the value of a^+_{0+} one can not draw a conclusion on the value for $a^+_3 = a^+_{0+} - a^-_{0+}$. In particular, the small value of $a^+_3 = 0.077/M_{\pi^+}$ found in ref.[35] is consistent within the bands given above. The resulting predictions for the S–wave scattering lengths in comparison to the pionic atom measurements are shown in fig. 6. Finally, the so–called subthreshold parameters are discussed in app. E.

Of course, one has to ask for the convergence. This issue is addressed for fit 1 in fig. 7 (the results for fits 2,3 are almost identical). In the S–waves, the second and third order contributions are small up to $q_\pi \simeq 100\,\mathrm{MeV}$. For higher energies, there are sizeable cancellations between the second and the third order. In the P–waves, the situation is somewhat different. While the first order describes well the partial waves P_{31} and P_{13},

there are sizeable second and third order contributions of opposite sign above approximately 70 MeV. For P_{11}, the same happens even at somewhat smaller momenta. Finally, in the case of the P_{33}, the third order terms contribute very little and the tail of the Δ is encoded in the second order contribution $\sim c_i$. For all partial waves we observe that the counterterm contribution is much bigger than the one from the tree graphs at that order. Note also that at third order, the loop and the c_i/m terms are much more important than the third order counterterm amplitude $\sim d_i$. This is the reason why these third order LECs can only be determined with a rather large uncertainty and vary from fit to fit (although they overlap within the error bars, cf. table 2). In light of these results, a fourth order calculation is called for. This conclusion was also reached in [12], where the convergence of the threshold parameters was studied.

4.3 Comparison to other calculations

First, we come back to the LECs c_i. These have been obtained in [11] by fitting threshold and subthreshold parameters as well as the σ–term. All the quantities considered in that paper did not depend on dimension three LECs. The value of c_1 we find is sizeably bigger than in [11], leading to a σ–term of 73.0, 88.2 and 96.4 MeV for fits 1,2,3, respectively. However, the fit to the phase shifts is not too sensitive to the value of c_1. Fixing its value as given in [11], corresponding to a σ–term of 47.6 MeV, the fit does only give a somewhat worse χ^2/dof for fits 1 and 3. For fit 2, the changes are more dramatic. In all cases, it is mostly the description of the S_{31} phase above 130 MeV that worsens. Clearly, a precise determination of c_1 from the phase shifts does not seem to be possible to this order. Note also that an order q^3 calculation is certainly not sufficient for the σ–term. This statement is underlined by the SU(3) calculation of the baryon masses and σ–terms to order q^4 presented in [36]. The values for the LECs $c_{2,3,4}$ are in good agreement with the values found in [11], only c_2 comes out slightly larger here. If one, however, fixes the values of the LECs to the previously determined values, the fits get clearly worse. We believe that the method employed here, namely to fit to various sets of phase shifts, gives a better handle on the theoretical uncertainties than the method used in [11]. A more consistent picture of the LEC c_1 will certainly emerge in a calculation at order q^4, which goes beyond the scope of this paper. Notice also that the combination $c^+ = c_2 + c_3 - 2c_1$, which enters directly the formula for the isoscalar S–wave scattering length, is very small in all cases. We find $c^+ = -0.20, +0.13, +0.08\,\mathrm{GeV}^{-1}$ for fits 1,2,3, respectively and of the same size than in [11, 34], where $c^+ = -0.09 \pm 0.37\,\mathrm{GeV}^{-1}$.

The results of ref.[12] are comparable for the LECs c_i but the resulting phase shifts deviate earlier from the data as shown in ref. [15]. This underlines our point that using only threshold parameters to fix the LECs is a less precise method. A better description of the phase shifts also at higher energies is, of course, achieved when one introduces the Δ–resonance explicitely in the effective Lagrangian. The most elaborate calculation in this respect is the one of Ellis and Tang [38, 39]. They employ a different counting scheme by expanding the relativistic pion–nucleon loop graphs. While this procedure might be legitimate at order q^3, it is not clear to us how one can systematically extend this scheme to higher orders since at some point it will face the same difficulties encountered by Gasser et al. [19] in the fully relativistic calculation. Furthermore, the inclusion of the

Δ–isobar is not done along the lines of a consistent power counting as outlined recently by Hemmert et al. [40]. The full complexity of consistently including the Δ can be seen from the renormalization of g_A as spelled out in [41]. While the approach of [39] is clearly superior for describing the phases up to higher energies, the amplitude we have constructed can certainly be controlled better in the extrapolation to and below the threshold. Furthermore, it can immediately be extended to include virtual photons [16]. The issue of isospin violation as evaluated in the consistent CHPT machinery, i.e. in an effective field theory including pions, nucleons and virtual photons, will be addressed in a forthcoming publication.

Acknowledgements

We are grateful to Gerhard Höhler, Evangelos Matsinos and Marcello Pavan for useful communications.

A Field transformations and the minimal Lagrangian

In this appendix, we will show how one can use field transformations to construct the minimal Lagrangian discussed in section 2. We consider relativistic spin-1/2 fields since we always construct first the minimal Lagrangian before performing the heavy fermion limit. Stated differently, our starting point is always the relativistic pion–nucleon theory which is mapped onto the heavy fermion limit by means of the path integral as spelled out in [17].

First, we will be concerned with the reduction of terms which are proportional to the mesonic equations of motion (eom) derived from the lowest order (dimension two) effective meson Lagrangian (note, however, that one can use this method also at higher orders, i.e. one does not have to start with the mesonic eom derived from $\mathcal{L}^{(2)}_{\pi\pi}$). The mesonic eom used here reads

$$2\,[iD_\mu, u^\mu] = \chi_- - \frac{1}{2}\langle\chi_-\rangle \ . \tag{A.1}$$

We will show now how one can systematically eliminate such terms. As an example, consider the possible scalar–isoscalar combination contributing to the effective pion–nucleon Lagrangian,

$$\bar\Psi\,\gamma_5\,[iD_\mu, u^\mu]\,\Psi \quad . \tag{A.2}$$

Such type of terms do not appear in the minimal form of the Lagrangian given in Eq.(2.31). To eliminate such a contribution, we redefine the U–field in the following way (note that U' denotes the field before the transformation subject to the conditions $(U')^\dagger U' = 1$ and $\det U' = 1$):

$$U = \exp\!\left\{-\frac{i}{2}\bar\Psi i\gamma_5\tau^i\Psi\; u\tau^i u^\dagger\right\} U' \ . \tag{A.3}$$

It is easy to check that the argument of the exponential is hermitean, i.e. we are dealing with a unitary transformation, $U^\dagger U = U U^\dagger = 1$. Furthermore, the property $\det U = 1$ has to be preserved. This follows from

$$\begin{aligned} \det U &= \det\left(\exp\left\{-\frac{i}{2}\bar\Psi i\gamma_5\tau^i\Psi\, u\tau^i u^\dagger\right\}\right)\det U' \\ &= \exp\left\{-\frac{i}{2}\bar\Psi i\gamma_5\tau^i\Psi\,\langle u\tau^i u^\dagger\rangle\right\} \\ &= 1\ , \end{aligned} \tag{A.4}$$

using $\langle u\tau^i u^\dagger\rangle = 0$ and $\det U' = 1$. Consequently, the lowest order meson Lagrangian takes the form

$$\begin{aligned} \mathcal{L}^{(2)}_{\pi\pi} &= \frac{F^2}{4}\langle D_\mu U D^\mu U^\dagger + \chi\, U^\dagger + U\,\chi^\dagger\rangle \\ &= \frac{F^2}{4}\langle D_\mu U' D^\mu (U')^\dagger + \chi\,(U')^\dagger + U'\,\chi^\dagger\rangle + \mathcal{L}^{(1)}_{\bar\Psi\Psi,\mathrm{induced}} + \mathcal{L}^{(1)}_{\bar\Psi\Psi\bar\Psi\Psi,\mathrm{induced}} + \dots\ . \end{aligned} \tag{A.5}$$

Note that such type of field redefinitions induce by construction a whole string with two, four, ... nucleon fields chirally coupled to pions and external sources. Here we are only interested in processes with exactly one nucleon line running through the pertinent Feynman diagrams. In this case, the induced term reads

$$\begin{aligned} \mathcal{L}^{(1)}_{\bar\Psi\Psi,\mathrm{induced}} &= i\frac{1}{2}\bar\Psi i\gamma_5\tau^i\Psi\langle\tau^i\chi_-\rangle + i\frac{1}{2}\bar\Psi i\gamma_5\tau^i\Psi\langle\tau^i[iD_\mu,u^\mu]\Psi \\ &= -\bar\Psi\gamma_5\chi_-\Psi + \frac{1}{2}\bar\Psi\gamma_5\langle\chi_-\rangle\Psi - \bar\Psi\gamma_5[iD_\mu,u^\mu]\Psi\ . \end{aligned} \tag{A.6}$$

The last term in Eq.(A.6) obviously cancels the one given in Eq.(A.2). The other terms in Eq.(A.6) can be eliminated by applying similar field transformations on the nucleon fields as discussed below. The multi–fermion terms not discussed here play, of course, a role in the construction of chiral invariant few–nucleon forces.

Consider now the nucleon eom terms. Be A an arbitrary local operator of chiral dimension two (or higher). We redefine the nucleon spinor via

$$\Psi = (1+\gamma_0 A^\dagger\gamma_0)\,\Psi'\ , \quad \bar\Psi = \bar\Psi'(1+A)\ . \tag{A.7}$$

This induces a string of additional terms in the leading order pion–nucleon Lagrangian,

$$\mathcal{L}^{(1)}_{\pi N} = \mathcal{L}^{(1\,\prime)}_{\pi N} + \mathcal{L}^{(1)}_{\pi N,\mathrm{induced}} \tag{A.8}$$

$$\begin{aligned} \mathcal{L}^{(1)}_{\pi N,\mathrm{induced}} &= \bar\Psi\left(-i\,\overleftarrow{\not D}\,\gamma_0 A^\dagger\gamma_0 + Ai\,\vec{\not D}\right)\Psi - m\bar\Psi(A+\gamma_0 A^\dagger\gamma_0)\Psi \\ &+ \frac{g_A}{2}\bar\Psi(A\,\not u\,\gamma_5 + \not u\,\gamma_5\gamma_0 A^\dagger\gamma_0)\Psi. \end{aligned} \tag{A.9}$$

As an example, consider the third order term

$$\mathcal{L}^{(3)}_{\pi N} = \bar\Psi\gamma_5\chi_-\Psi + \dots\ , \tag{A.10}$$

which is exactly the structure that appeared before. With $A = \gamma_5\chi_-/(2m)$, we have

$$\Psi = \Big(1 + \frac{1}{2m}\gamma_5\chi_-\Big)\,\Psi' \ , \quad \bar\Psi = \bar\Psi'\Big(1 + \frac{1}{2m}\gamma_5\chi_-\Big) \ , \tag{A.11}$$

so that

$$\begin{aligned}
\mathcal{L}^{(3)}_{\pi N,\rm induced} &= \frac{1}{2m}\bar\Psi'\Big(-i\stackrel{\leftarrow}{\not D}\,\gamma_5\chi_- + \gamma_5\chi_- i\stackrel{\rightarrow}{\not D}\Big)\Psi' - \bar\Psi'\gamma_5\chi_-\Psi - \frac{g_A}{4m}\bar\Psi'\gamma_\mu[\chi_-,u^\mu]\Psi' \\
&= -\bar\Psi'\gamma_5\chi_-\Psi + \frac{1}{2m}\bar\Psi'\gamma_\mu\gamma_5[D_\mu,\chi_-]\Psi' - \frac{g_A}{4m}\bar\Psi'\gamma_\mu[\chi_-,u^\mu]\Psi' \ . \qquad \text{(A.12)}
\end{aligned}$$

Therefore, the term in Eq.(A.10) is cancelled by the first term of the induced Lagrangian. Notice that this is equivalent to the relation Eq.(2.29) but derived simply by field redefinitions. In a similar fashion, one can construct other operators A which then lead to all other relations given in Eqs.(2.22-2.30).

B Reduction of the Clifford–algebra in HBCHPT

In this appendix, we collect the various expressions of the γ matrices expressed in terms of the nucleon four–velocity and the covariant spin–operator. Consider first $\bar HH$ matrix elements:

$$\begin{aligned}
\bar HH &= \bar HH \ , && \text{(B.1)}\\
\bar H\gamma_\mu H &= v_\mu \bar HH \ , && \text{(B.2)}\\
\bar H\gamma_5 H &= 0 \ , && \text{(B.3)}\\
\bar H\gamma_\mu\gamma_5 H &= 2\,\bar HS_\mu H \ , && \text{(B.4)}\\
\bar H\sigma_{\mu\nu} H &= 2\,\epsilon_{\mu\nu\alpha\beta}v^\alpha \bar HS^\beta H \ , && \text{(B.5)}\\
\bar H\gamma_5\sigma_{\mu\nu} H &= 2i\,\bar H(v_\mu S_\nu - v_\nu S_\mu)H \ . && \text{(B.6)}
\end{aligned}$$

Similarly, $\bar hH$ matrix elements reduce to

$$\begin{aligned}
\bar hH &= 0 \ , && \text{(B.7)}\\
\bar h\gamma_\mu H &= \bar h(\gamma_\mu - v_\mu)H \ , && \text{(B.8)}\\
\bar h\gamma_5 H &= \bar h\gamma_5 H \ , && \text{(B.9)}\\
\bar h\gamma_\mu\gamma_5 H &= -v_\mu\bar h\gamma_5 H \ , && \text{(B.10)}\\
\bar h\sigma_{\mu\nu} H &= -i\,\bar h(v_\mu\gamma_\nu - v_\nu\gamma_\mu)H \ , && \text{(B.11)}\\
\bar h\gamma_5\sigma_{\mu\nu} H &= -\epsilon_{\mu\nu\alpha\beta}v^\alpha\bar h\gamma^\beta H \ . && \text{(B.12)}
\end{aligned}$$

The ones for $\bar Hh$ are identical, only the last three expressions have a plus sign on the right hand side. Finally, we list some of the operators which appear when performing the $1/m$ expansion of the generating functional:

$$\begin{aligned}
\bar H(\gamma_\mu - v_\mu)(\gamma_\nu - v_\nu)H &= \bar H(g_{\mu\nu} - v_\mu v_\nu - 2[S_\mu,S_\nu])H \ , && \text{(B.13)}\\
\bar H(\gamma_\mu - v_\mu)\gamma_5 H &= 2\,\bar HS_\mu H \ , && \text{(B.14)}\\
\bar H\gamma_5(\gamma_\mu - v_\mu)H &= -2\,\bar HS_\mu H \ , && \text{(B.15)}\\
\bar H(\gamma_\mu - v_\mu)S_\nu\gamma_5 H &= -1/2\,\bar H(g_{\mu\nu} - v_\mu v_\nu - 2[S_\mu,S_\nu])H \ , && \text{(B.16)}\\
\bar H\gamma_5 S_\nu(\gamma_\mu - v_\mu)H &= 1/2\,\bar H(g_{\mu\nu} - v_\mu v_\nu + 2[S_\mu,S_\nu])H \ , && \text{(B.17)}\\
\bar H(\gamma_\mu - v_\mu)S_\nu(\gamma_\lambda - v_\lambda)H &= \bar H(-i/2\,\epsilon_{\mu\nu\lambda\alpha}v^\alpha + (g_{\mu\nu} - v_\mu v_\nu)S_\lambda \\
&\quad -(g_{\mu\lambda} - v_\mu v_\lambda)S_\nu + (g_{\nu\lambda} - v_\nu v_\lambda)S_\mu)H \ . && \text{(B.18)}
\end{aligned}$$

C Feynman rules from the third order Lagrangian

In this appendix, we give the Feynman rules needed to work out πN scattering based on the Lagrangian, Eq.(2.44). We use the following conventions: The momenta p_1 and q_1 are always *in*coming, whereas p_2, q_2 and q (the latter is the pion momentum in case of the πN vertex) are always *out*going. Also, 'a, b, c' are pion isospin indices. Consider first the contributions from the terms with *fixed* coefficients (this includes the terms which are $1/m$–corrections to dimension two operators with LECs c_i):

Nucleon kinetic energy

$$i\frac{(v\cdot p_1)^3-(v\cdot p_1)\,p_1^2}{4m^2}\ ; \tag{C.1}$$

one pion

$$\begin{aligned}-\frac{g_A}{4m^2F}\quad &\Big\{\frac{1}{2}S\cdot q q^2+S\cdot q v\cdot p_1 v\cdot p_2-v\cdot(p_1+p_2)S\cdot(p_1+p_2)v\cdot q\\ &-\frac{1}{2}S\cdot q(p_1^2+p_2^2)+[S\cdot p_2 q\cdot p_1+S\cdot p_1 q\cdot p_2]\Big\}\,\tau^a\ ;\end{aligned} \tag{C.2}$$

two pions

$$\begin{aligned}i\,\frac{\delta^{ab}}{F^2}\quad &\Big\{\frac{g_A^2}{16m^2}[3v\cdot q_1 v\cdot q_2 v\cdot(p_1+p_2)-v\cdot q_1 q_2\cdot(p_1+p_2)-v\cdot q_2 q_1\cdot(p_1+p_2)]\\ &+\frac{c_2}{m}[v\cdot q_1 q_2\cdot(p_1+p_2)+v\cdot q_2 q_1\cdot(p_1+p_2)]\\ &+\frac{g_A^2}{8m^2}[S\cdot q_1,S\cdot q_2]v\cdot(q_1+q_2)\Big\}\\ -\frac{\epsilon^{bac}\,\tau^c}{8m^2F^2}\quad &\Big\{\frac{1}{2}v\cdot(q_1+q_2)[(v\cdot p_1)^2+(v\cdot p_2)^2+v\cdot p_1 v\cdot p_2]\\ &-\frac{1}{4}[(p_1^2+p_2^2)v\cdot(q_1+q_2)+v\cdot(p_1+p_2)(p_1+p_2)\cdot(q_1+q_2)]\\ &+[S\cdot q_1,S\cdot q_2]\,v\cdot(p_1+p_2)\\ &+(1+g_A^2+8mc_4)\,[v\cdot q_2 S\cdot q_1-v\cdot q_1 S\cdot q_2,S\cdot(p_1+p_2)]\\ &-\frac{g_A^2}{2}[v\cdot q_2 q_1(p_1-p_2)+v\cdot q_1 q_2(p_2-p_1)-v\cdot q_1 v\cdot q_2 v\cdot(q_1+q_2)]\\ &+\frac{1}{2}(1+8mc_4)\,[v\cdot q_1 q_2^2+v\cdot q_2 q_1^2-q_1 q_2 v\cdot(q_1+q_2)]\Big\}\ .\end{aligned} \tag{C.3}$$

Similarly, for the terms with LECs from $\mathcal{L}_{\pi N}^{(3)}$, we get:

Nucleon kinetic energy

$$-i\tilde{d}_{24}(\lambda)(v\cdot p_1)^3+8iM^2\tilde{d}_{28}(\lambda)(v\cdot p_1)\ ; \tag{C.4}$$

one pion

$$\begin{aligned}&\frac{2M^2}{F}[2d_{16}(\lambda)-d_{18}]S\cdot q\tau^a\\ &+\frac{1}{F}[\tilde{d}_{25}(\lambda)v\cdot p_1 v\cdot p_2+\tilde{d}_{29}(\lambda)(v\cdot q)^2]S\cdot q\tau^a\ ;\end{aligned} \tag{C.5}$$

two pions

$$
\begin{aligned}
i\,\frac{2\delta^{ab}}{F^2} \quad & \Big\{[-d_{14}(\lambda)+d_{15}][S\cdot q_1, S\cdot q_2]v\cdot(q_1+q_2) \\
& +2[\tilde{d}_{26}(\lambda)q_1\cdot q_2+\tilde{d}_{27}(\lambda)v\cdot q_1 v\cdot q_2-\tilde{d}_{28}(\lambda)M^2]v\cdot(p_1+p_2)\Big\} \\
-\frac{2\epsilon^{bac}\,\tau^c}{F^2} \quad & \Big\{(d_1(\lambda)+d_2(\lambda))q_1\cdot q_2+d_3(\lambda)\,v\cdot q_1 v\cdot q_2 \\
& +\Big[2M^2 d_5(\lambda)-\frac{1}{8}\tilde{d}_{24}(\lambda)[(v\cdot p_1)^2+(v\cdot p_2)^2+v\cdot p_1 v\cdot p_2] \\
& +M^2\tilde{d}_{28}(\lambda)\Big]v\cdot(q_1+q_2)+2\tilde{d}_{30}(\lambda)[S\cdot q_1, S\cdot q_2]\,v\cdot(p_1+p_2)\Big\}\ . \qquad \text{(C.6)}
\end{aligned}
$$

D Kinematics of pion–nucleon scattering

We consider the πN-scattering amplitude without assuming isospin symmetry (which is necessary if one wants to address isospin violation)[#13]

$$\pi(q_1)+N(p_1)\to\pi(q_2)+N(p_2)\ . \qquad \text{(D.1)}$$

Here $\pi(q_i)$ denotes a pion state in the physical basis (π^0,π^+,π^-) with four–momentum q_i and N a proton (p) or a neutron (n) with four–momentum p_i. The masses of the in(out)–going nucleon and pion are denoted by $m_{1(2)}$ and $M_{1(2)}$, respectively. Consider the center-of-mass system (cms) with $\vec{p}_i=-\vec{q}_i$, $i=1,2$. For the initial nucleon in the heavy fermion approach, we set $p_1=m_1\,v_1+k_1$ with $k_1\cdot p_1\ll m_1$. The pion and the nucleon energy in the in–state are (we use $v_1=(1,0,0,0)$)

$$\omega_1=v_1\cdot q_1=\sqrt{M_1^2+\vec{q}_1^{\,2}}\ ,\quad E_1=\sqrt{m_1^2+\omega_1^2-M_1^2}\ , \qquad \text{(D.2)}$$

in order. The energy of the out–going pion and nucleon reads

$$\omega_2=\frac{(E_1+\omega_1)^2+M_2^2-m_2^2}{2(E_1+\omega_1)}\ ,\quad E_2=E_1+\omega_1-\omega_2\ \ , \qquad \text{(D.3)}$$

respectively. Furthermore, the invariant momentum squared is

$$
\begin{aligned}
t=(q_1-q_2)^2 &= M_1^2+M_2^2-2\omega_1\omega_2+2\vec{q}_1\cdot\vec{q}_2 \\
&= M_1^2+M_2^2-2\omega_1\omega_2+2|\vec{q}_1||\vec{q}_2|\cos(\theta)\ , \qquad \text{(D.4)}
\end{aligned}
$$

and $\cos(\theta)\equiv z$ in the following. For the equal mass case ($M_1=M_2=M_\pi$, $m_1=m_2=m_N$), it is convenient to use the pion kinetic energy in the cms given by

$$T_\pi=\omega_{\rm cms}-M_\pi\quad , \qquad \text{(D.5)}$$

[#13]The reduction of these formulae to the isospin–conserving case is obvious.

and the pion three–momentum in the lab system, called $\vec{q}_\pi$, with norm q_π,

$$q_\pi = \sqrt{\frac{1}{4m^2}(s - M_\pi^2 - m_N^2)^2 - M_\pi^2} \ . \tag{D.6}$$

For example, $T_\pi = 50\,\mathrm{MeV}$ is equivalent to $q_\pi = 155.4\,\mathrm{MeV}$. For later use, we also need the following products involving the nucleon spinors (again written for the general case)

$$\bar{u}(p_2)\,u(p_1) = \mathcal{N}_1\mathcal{N}_2\left[1 - \frac{\vec{q}_1\cdot\vec{q}_2}{(E_1+m_1)(E_2+m_2)} + \frac{i\sigma\cdot(\vec{q}_1\times\vec{q}_2)}{(E_1+m_1)(E_2+m_2)}\right] , \tag{D.7}$$

$$\begin{aligned}\bar{u}(p_2)\,\not{q}_1\,u(p_1) &= \mathcal{N}_1\mathcal{N}_2\Big[\omega_1 + \frac{\vec{q}_1^{\,2}}{E_1+m_1} + \frac{\vec{q}_1\cdot\vec{q}_2}{E_2+m_2}\Big(1+\frac{\omega_1}{E_1+m_1}\Big) \\ &\quad - \frac{i\sigma\cdot(\vec{q}_1\times\vec{q}_2)}{E_2+m_2}\Big(1+\frac{\omega_1}{E_1+m_1}\Big)\Big] ,\end{aligned} \tag{D.8}$$

where the $\mathcal{N}_i$ are the conventional normalization factors,

$$\mathcal{N}_i = \sqrt{\frac{E_i+m_i}{2m_i}} \ , \quad i = 1,2 \ . \tag{D.9}$$

E Subthreshold parameters

In this appendix, we consider the expansion of the standard invariant pion–nucleon amplitudes with the pseudovector Born terms subtracted (as indicated by the "bar")

$$\bar{X} = \sum_{m,n} x_{mn}\,\nu^{2m+k}\,t^n \ , \quad X = \{A^\pm, B^\pm\} \ , \tag{E.1}$$

with

$$\nu = \frac{t}{4m} + \frac{1}{m}\Big(\omega^2 - M^2 + \omega\sqrt{m^2+\omega^2-M^2}\Big) \ , \tag{E.2}$$

and $k = 1\,(0)$ if the function considered is odd (even) in ν. Instead of the amplitudes $B^\pm$, we choose to work with $D^\pm = A^\pm + \nu\,B^\pm$. In particualr, the B^+ amplitude is dominated by the $\Delta(1232)$ and can only be expected to described well in a fourth order calculation. The invariant amplitudes $A^\pm$ and $B^\pm$ can be reconstructed from the $g^\pm, h^\pm$ amplitudes used throughout the main body of the paper via

$$A^\pm = C_1\,g^\pm + C_2\,h^\pm \ , \quad B^\pm = C_3\,g^\pm + C_4\,h^\pm \ , \tag{E.3}$$

with

$$\begin{aligned} C_1 &= \frac{\sqrt{s}+m}{2\sqrt{s}} \ , \ C_2 = -\frac{1}{2\sqrt{s}}\Big((\omega^2-M^2)\frac{2E\sqrt{s}-2m^2}{E-m} + (\sqrt{s}+m)\frac{t}{2}\Big) \ , \\ C_3 &= \frac{1}{2\sqrt{s}} \ , \ C_4 = \frac{1}{2\sqrt{s}}\Big((\omega^2-M^2)\frac{2m}{E-m} - \frac{t}{2}\Big) \ . \end{aligned} \tag{E.4}$$

Parameter	Fit 1	Fit 2	Fit 3	KH-analysis
$a^+_{00}[M_\pi^{-1}]$	-1.57	-1.27	-1.35	-1.46 ± 0.10
$a^+_{10}[M_\pi^{-3}]$	9.10	9.06	9.17	4.66
$a^+_{01}[M_\pi^{-3}]$	1.37	1.34	1.45	1.14 ± 0.02
$a^+_{11}[M_\pi^{-5}]$	0.07	0.07	0.07	-0.01
$d^+_{10}[M_\pi^{-3}]$	1.23	1.14	1.19	1.12 ± 0.02
$d^+_{01}[M_\pi^{-3}]$	1.37	1.34	1.45	1.14 ± 0.02
$a^-_{00}[M_\pi^{-2}]$	-8.47	-8.88	-8.73	-8.83 ± 0.10
$a^-_{10}[M_\pi^{-4}]$	-1.45	-1.36	-1.43	-1.25 ± 0.05
$a^-_{01}[M_\pi^{-4}]$	-0.46	-0.48	-0.43	-0.37 ± 0.02
$a^-_{11}[M_\pi^{-6}]$	0.0	0.0	0.0	0.01 ± 0.01
$d^-_{00}[M_\pi^{-2}]$	1.87	1.59	1.80	1.53 ± 0.02
$d^-_{10}[M_\pi^{-4}]$	-0.65	-0.56	-0.63	-0.17 ± 0.01
$d^-_{01}[M_\pi^{-4}]$	-0.32	-0.34	-0.29	-0.13 ± 0.01

Table 4: Subthreshold parameters for the $A^\pm$ and $D^\pm$ amplitudes for the three fits in comparison to the Karlsruhe-Helsinki analysis.

It is now straightforward to work out the subthreshold expansion around $\nu = t = 0$. Here, we collect the results for the coefficients of the subthreshold expansion which involve only lower powers in t and/or ν and are accessible in a q^3 calculation (see also app. A of [11] for some additional results). We find (we only give the formulas for the subthreshold parameters not already given in [11]):

$$a^+_{10} = \frac{1}{8F_\pi^4\pi^2}\left[16F_\pi^2\pi^2 c_2 - 32mF_\pi^2\pi^2(\bar{d}_{14}-\bar{d}_{15}) + mg_A^4\right] - \frac{M_\pi}{8\pi F_\pi^4}\left[\frac{5g_A^2}{4}+1\right], \tag{E.5}$$

$$\begin{aligned} a^-_{00} &= -\frac{2mc_4}{F_\pi^2} + \frac{M_\pi m g_A^2(1+g_A^2)}{8\pi F_\pi^4} \\ &+ \frac{M_\pi^2}{48m^2F_\pi^4\pi^2}\left[g_A^4 m^2 + 6F_\pi^2\pi^2(1-4mc_4+32m^2(\bar{d}_1+\bar{d}_2)+64m^2\bar{d}_5)\right], \end{aligned} \tag{E.6}$$

$$a^-_{10} = -\frac{mg_A^4}{32\pi F_\pi^4 M_\pi} - \frac{1}{240m^2F_\pi^4\pi^2}\left[(15+7g_A^4)m^2 + 30F_\pi^2\pi^2(1-4mc_4+32m^2\bar{d}_3)\right], \tag{E.7}$$

$$a^-_{01} = -\frac{mg_A^2}{96\pi F_\pi^4 M_\pi} - \frac{1}{192mF_\pi^4\pi^2}\left[(1+7g_A^2+2g_A^4)m + 48F_\pi^2\pi^2(-c_4+8m(\bar{d}_1+\bar{d}_2))\right], \tag{E.8}$$

$$d^-_{00} = \frac{1}{2F_\pi^2} + \frac{M_\pi^2}{48\pi^2F_\pi^4}\left[g_A^4 + 192F_\pi^2\pi^2(\bar{d}_1+\bar{d}_2+2\bar{d}_5)\right], \tag{E.9}$$

$$d_{10}^- = -\frac{1}{240\pi^2 F_\pi^4}\left[15 + 7g_A^4 - 960F_\pi^2\pi^2\bar{d}_3\right] , \tag{E.10}$$

$$d_{01}^- = -\frac{1}{192\pi^2 F_\pi^4}\left[1 + 7g_A^2 + 2g_A^4 + 384F_\pi^2\pi^2(\bar{d}_1 + \bar{d}_2)\right] . \tag{E.11}$$

Notice that $d_{0n}^+ = a_{0n}^+$ for any n. The resulting values are given in table 4. The "empirical" values based on a dispersion–theoretical continuation into the unphysical region are taken from [28]. For the VPI SP98 analysis, we have in addition [32]

$$d_{00}^+ = -1.30\, M_\pi^{-1} , \quad d_{01}^+ = 1.27\, M_\pi^{-3} . \tag{E.12}$$

Obviously, only in some cases the one-loop result is in good agreement with the empirical values as deduced from the Karlsruhe–Helsinki (KH) phase shift analysis. Note, however, that recent low energy πN-scattering data from PSI [42] (see also ref.[29]) show some disagreement with the KH80 solution of πN dispersion analysis. It therefore seems necessary to redo the πN-dispersion analysis with the inclusion of these new data. This was done partly in the VPI SP98 analysis leading e.g. to the values of the two subthreshold parameters quoted in Eq.(E.12). However, a full–scale dispersive reanalysis for all (sub)threshold parameters is not yet available.

References

[1] D. Chatellard et al., Phys. Rev. Lett. 74 (1995) 4157;
D. Sigg et al., Phys. Rev. Lett. 75 (1995) 3245;
D. Sigg et al., Nucl. Phys. A609 (1996) 269, (E) A617 (1997) 526.

[2] M. Fuchs et al., Phys. Lett. B368 (1996) 20.

[3] J. Bergstrom et al., Phys. Rev. C53 (1996) R1052.

[4] W.R. Gibbs, Li Ai and W.B. Kaufmann, Phys. Rev. Lett. 74 (1995) 3740.

[5] E. Matsinos, Phys. Rev. C58 (1997) 3014.

[6] V. Bernard, N. Kaiser and Ulf-G. Meißner, Int. J. Mod. Phys. E4 (1995) 193.

[7] Ulf-G. Meißner, Lectures given at 12th Annual HUGS at CEBAF, Newport News, VA, USA, 2-20 June, 1997 [hep-ph/9711365].

[8] V. Bernard, N. Kaiser and Ulf-G. Meißner, Phys. Lett. B309 (1993) 421.

[9] V. Bernard, N. Kaiser and Ulf-G. Meißner, Phys. Rev. C52 (1995) 2185.

[10] V. Bernard, N. Kaiser and Ulf-G. Meißner, Phys. Lett. B389 (1996) 144.

[11] V. Bernard, N. Kaiser and Ulf-G. Meißner, Nucl. Phys. A615 (1997) 483.

[12] M. Mojžiš, Eur. Phys. J. C2 (1998) 181.

[13] G. Ecker and M. Mojžiš, Phys. Lett. B365 (1996) 312.

[14] R. Koch and E. Pietarinen, Nucl. Phys. A336 (1980) 331.

[15] A. Datta and S. Paksava, Phys. Rev. D56 (1997) 4322.

[16] Ulf-G. Meißner and S. Steininger, Phys. Lett. B419 (1998) 403.

[17] V. Bernard, N. Kaiser, J. Kambor and Ulf-G. Meißner, Nucl. Phys. B388 (1992) 315.

[18] Ulf-G. Meißner, G. Müller and S. Steininger, Phys. Lett. B406 (1997) 154;
(E) *ibid* B407 (1997) 154.

[19] J. Gasser, M.E. Sainio and A. Švarc, Nucl. Phys. B307 (1988) 779.
[20] S. Steininger, Ph.D. thesis, University of Bonn, in preparation.
[21] E. Jenkins and A.V. Manohar, Phys. Lett. B255 (1991) 558.
[22] G. Ecker, Phys. Lett. B336 (1994) 508.
[23] G. Müller and Ulf-G. Meißner, Nucl. Phys. B492 (1997) 379.
[24] J. Gasser and Ulf-G. Meißner, Phys. Lett. B258 (1991) 219.
[25] V. Bernard, N. Kaiser and Ulf-G. Meißner, Z. Phys. C70 (1996) 483.
[26] G. Ecker and M. Mojžiš, Phys. Lett. B410 (1997) 266.
[27] V. Bernard, N. Kaiser and Ulf-G. Meißner, Nucl. Phys. B457 (1995) 147.
[28] G. Höhler, in Landolt-Börnstein, Vol. 9b2, ed H. Schopper (Springer, Berlin, 1983).
[29] Proccedings of the Seventh International Symposium on Meson–Nucleon Physics and the Structure of the Nucleon, published in πN Newsletter 13 (1997) 1-398.
[30] R. Koch, Nucl. Phys. A448 (1986) 707.
[31] E. Matsinos, Phys. Rev. C56 (1997) 3014; E. Matsinos, private communication.
[32] SAID on-line program, R.A. Arndt, R.L. Workman et al., see website http://clsaid.phys.vt.edu/ CAPS/.
[33] J. Gasser, H. Leutwyler and M.E. Sainio, Phys. Lett. B253 (1991) 252, 260.
[34] S.R. Beane, V. Bernard, T.S.H. Lee and Ulf-G. Meißner, Phys. Rev. C57 (1998) 424.
[35] N. Fettes and E. Matsinos, Phys. Rev. C55 (1997) 464.
[36] B. Borasoy and Ulf-G. Meißner, Ann. Phys. (NY) 254 (1997) 192.
[37] P.F.A. Goudsmit, H.J. Leisi, E. Matsinos, B.L. Birbrair and A.B. Gridnev, Nucl. Phys. A575 (1994) 673.
[38] P.J. Ellis and H.-B. Tang, Phys. Rev. C56 (1997) 3363.
[39] P.J. Ellis and H.-B. Tang, Phys. Rev. C57 (1998) 3356.
[40] T.R. Hemmert, B.R. Holstein and J. Kambor, Phys. Lett. B395 (1997) 89.
[41] V. Bernard, H.W. Fearing, T.R. Hemmert and Ulf-G. Meißner, Nucl. Phys. A635 (1998) 121.
[42] Ch. Joram et al., Phys. Rev. C51 (1995) 2144, 2159.
[43] R. Baur and J. Kambor, [hep-ph/9803311].
[44] S. Steininger, Ulf-G. Meißner and N. Fettes, [hep-ph/9808280].

Figures

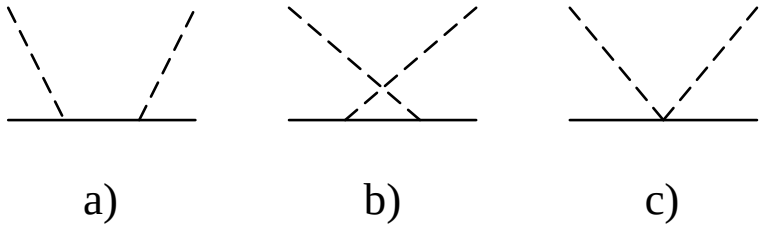

Figure 1: Tree graphs in the relativistic approach as discussed in the text.

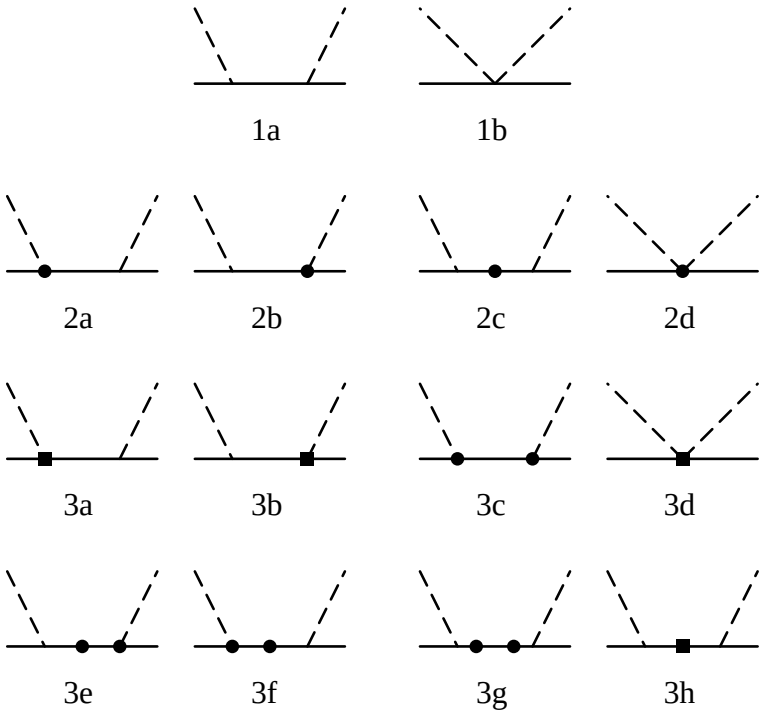

Figure 2: Tree graphs in the heavy baryon approach. The heavy dots refer to insertions from $\mathcal{L}_{\pi N}^{(2)}$ and the filled squares to insertions from $\mathcal{L}_{\pi N}^{(3)}$.

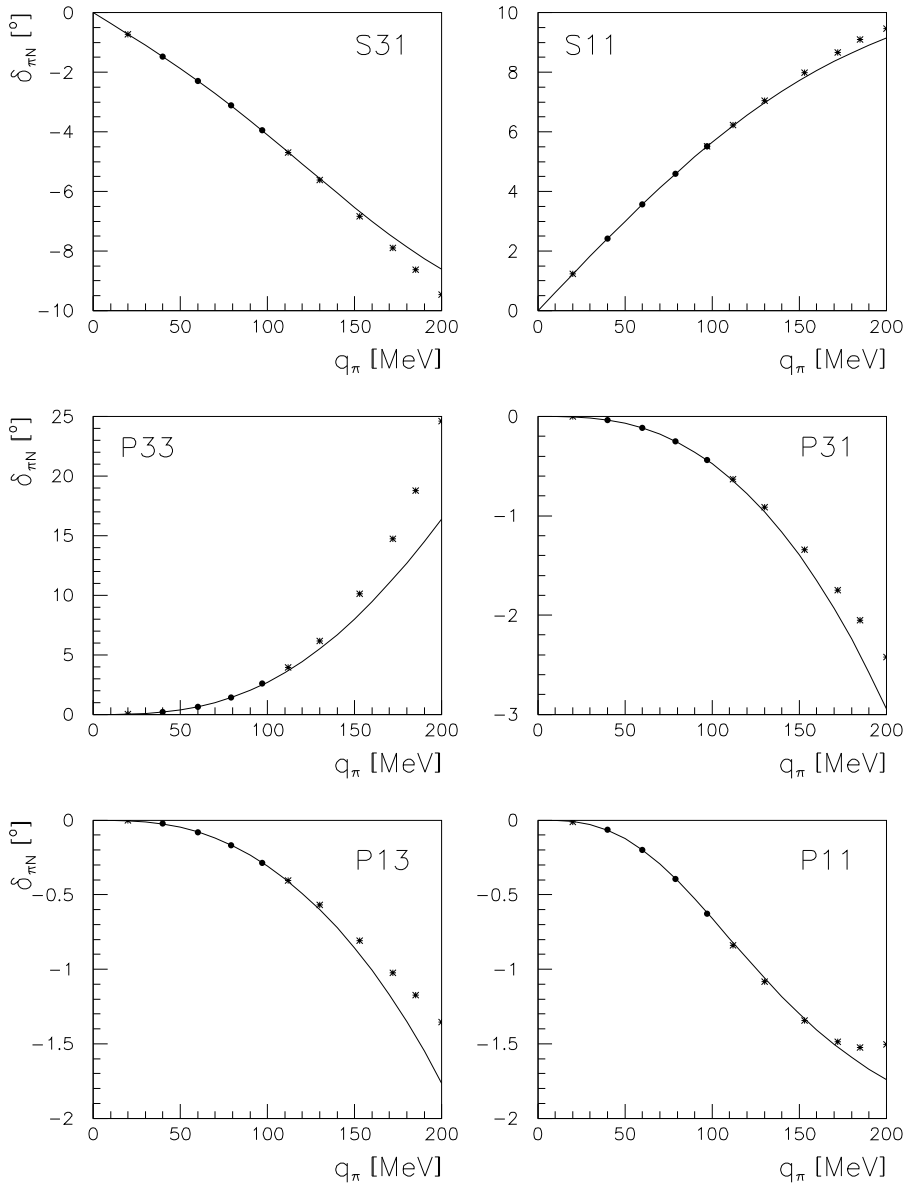

Figure 3: Fits and predictions for the KA85 phase shifts as a function of the pion laboratory momentum q_π. Fitted in each partial wave are the data between 40 and 97 MeV (filled circles). For higher and lower energies, the phases are predicted.

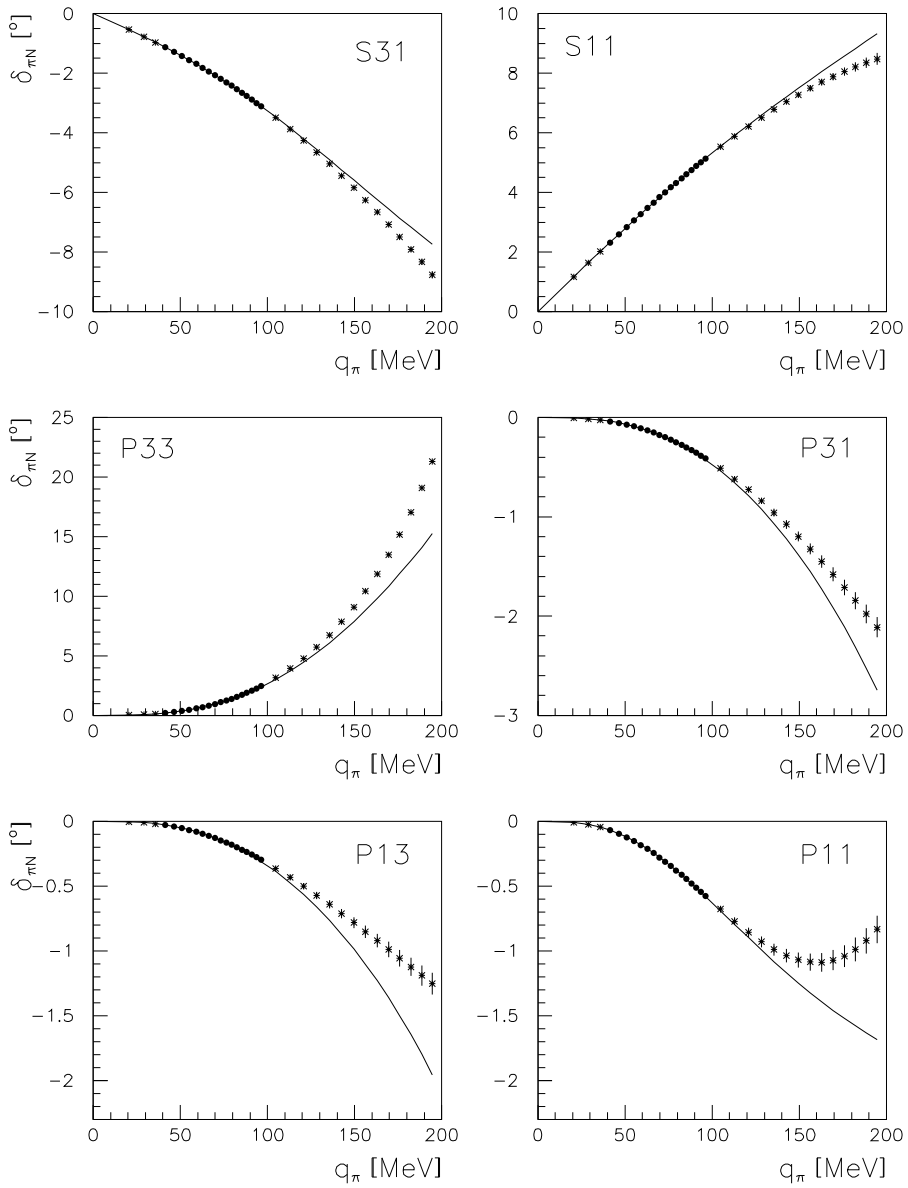

Figure 4: Fits and predictions for the EM98 phase shifts as a function of q_π. Fitted in each partial wave are the data between 41 and 97 MeV (filled circles). For higher and lower energies, the phases are predicted as shown by the solid lines.

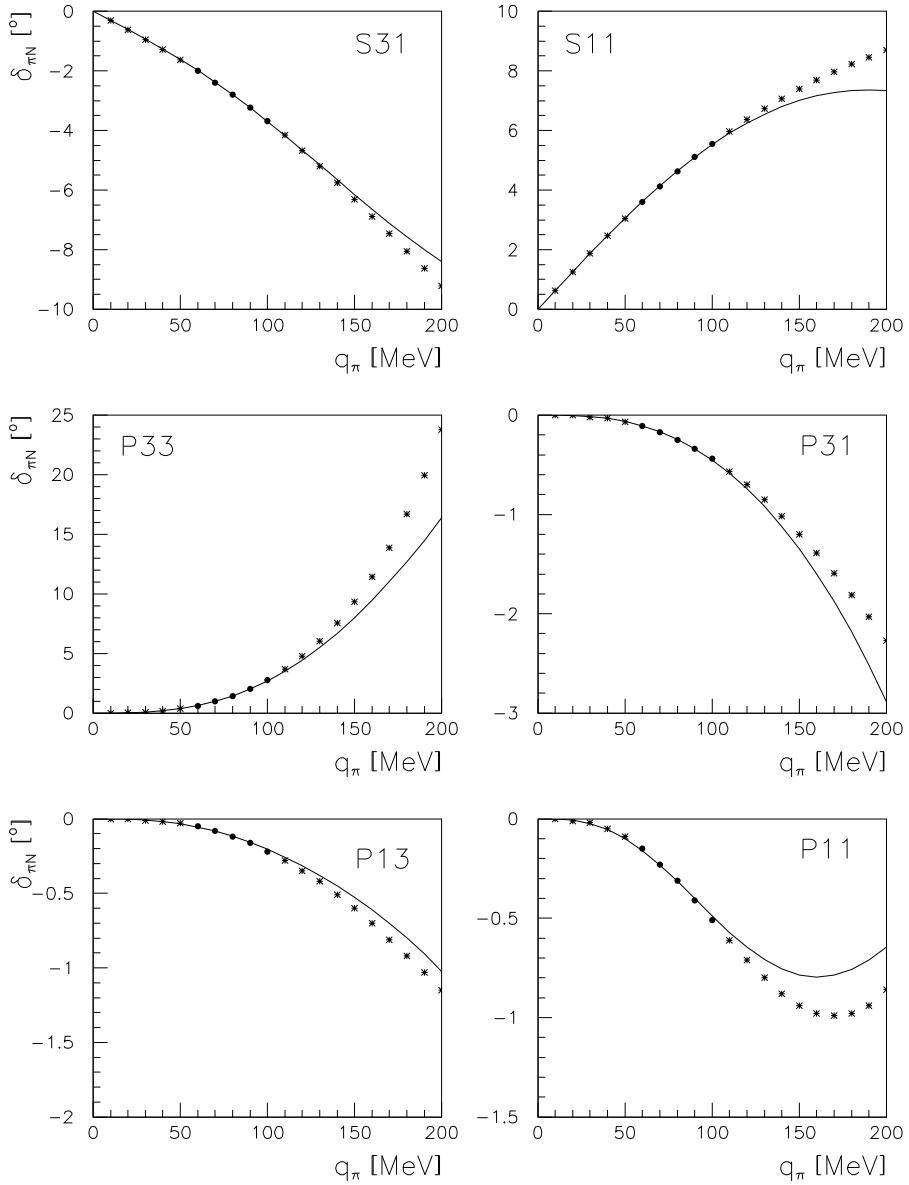

Figure 5: Fits and predictions for the SP98 phase shifts as a function of the pion laboratory momentum q_π. Fitted in each partial wave are the data between 60 and 100 MeV (filled circles). For higher and lower energies, the phases are predicted as shown by the solid lines.

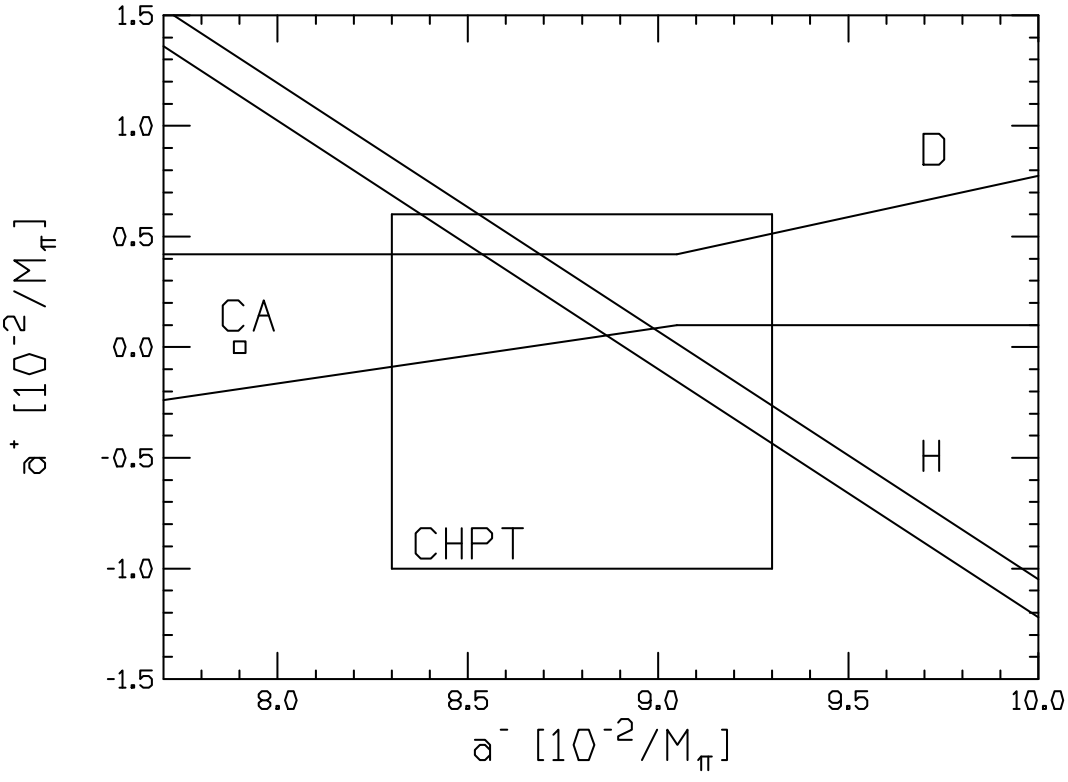

Figure 6: S–wave scattering lengths. Shown are the results obtained from the level shift in pionic hydrogen (H–band) and pionic deuterium (D–band) compared to the current algebra (CA) and order q^3 CHPT prediction.

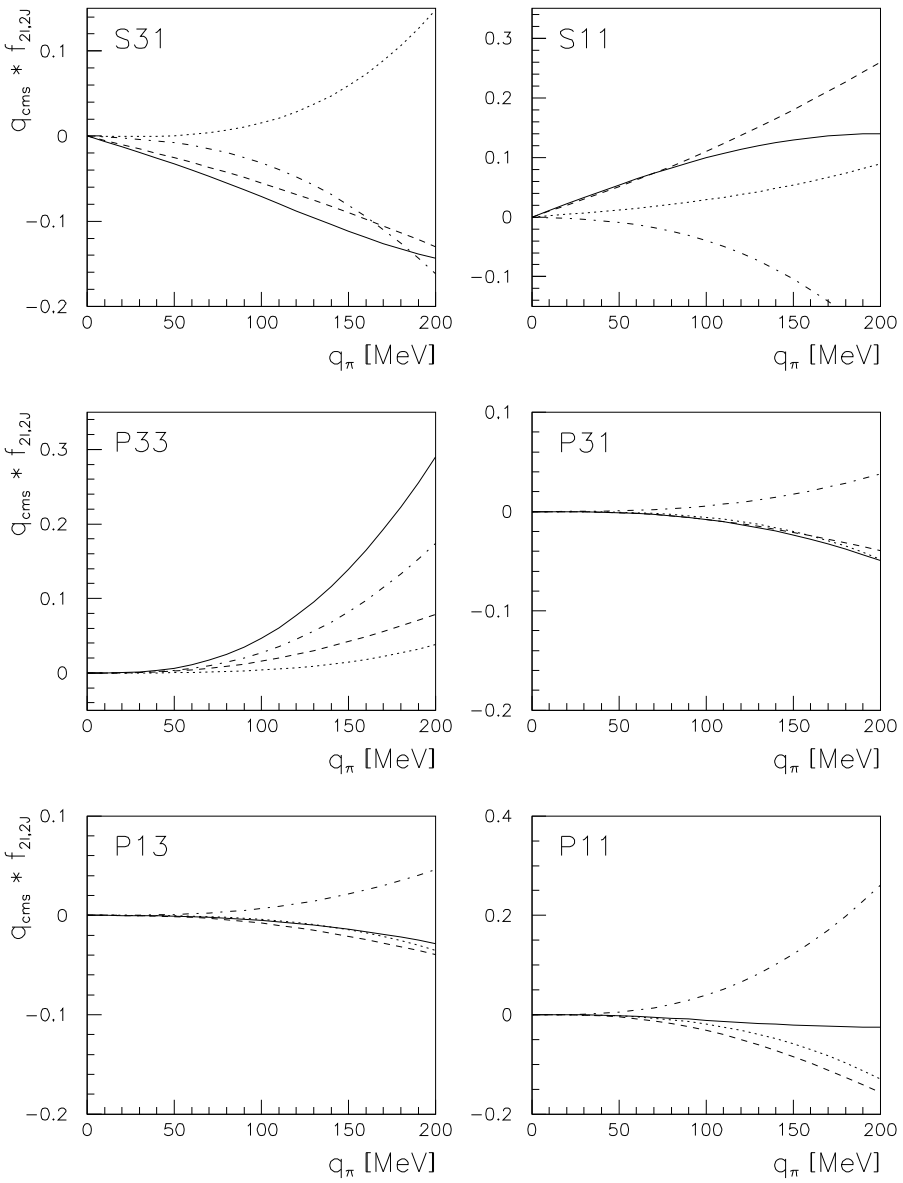

Figure 7: Convergence properties as exemplified by the KA85 partial wave amplitudes. Shown are the real part of the amplitudes multiplied by the modulus of the pion cm momentum. The dashed, dashed–dotted and dotted lines give the first, second and third order, respectively. The sum is depicted by the solid lines.